doi:10.1111/evo.13715

A multiple peak adaptive landscape based on feeding strategies and roosting ecology shaped the evolution of cranial covariance structure and morphological differentiation in phyllostomid bats

Daniela M. Rossoni,[1,2] Bárbara M. A. Costa,[1] Norberto P. Giannini,[3] and Gabriel Marroig[1]

[1]*Department of Genetics and Evolutionary Biology, Biosciences Institute, University of São Paulo, São Paulo, Brazil*

[2]*E-mail: daniela.rossoni@gmail.com*

[3]*Unidad Ejecutora Lillo-CONICET, Universidad Nacional de Tucumán, San Miguel de Tucumán, Argentina*

Received December 2, 2016

Accepted February 15, 2019

We explored the evolution of morphological integration in the most noteworthy example of adaptive radiation in mammals, the New World leaf-nosed bats, using a massive dataset and by combining phylogenetic comparative methods and quantitative genetic approaches. We demonstrated that the phenotypic covariance structure remained conserved on a broader phylogenetic scale but also showed a substantial divergence between interclade comparisons. Most of the phylogenetic structure in the integration space can be explained by splits at the beginning of the diversification of major clades. Our results provide evidence for a multiple peak adaptive landscape in the evolution of cranial covariance structure and morphological differentiation, based upon diet and roosting ecology. In this scenario, the successful radiation of phyllostomid bats was triggered by the diversification of dietary and roosting strategies, and the invasion of these new adaptive zones lead to changes in phenotypic covariance structure and average morphology. Our results suggest that intense natural selection preceded the invasion of these new adaptive zones and played a fundamental role in shaping cranial covariance structure and morphological differentiation in this hyperdiverse clade of mammals. Finally, our study demonstrates the power of combining comparative methods and quantitative genetic approaches when investigating the evolution of complex morphologies.

KEY WORDS: **Adaptive radiation, macroevolution, multi-peaked adaptive landscapes, phyllostomidae, phylogenetic comparative methods, quantitative genetics.**

In evolutionary quantitative genetics, the genetic variance–covariance matrix (G-matrix) is a key parameter in understanding the pace, rate, and trajectory of multivariate evolution (Lande 1979; Lande and Arnold 1983; Schluter 1996). The G-matrix is particularly useful when describing complex morphologies and quantifying evolutionary changes, providing information on the amount of variation in single traits, as well as the extent to which a set of quantitative traits are genetically correlated (Lande and Arnold 1983). Estimating a G-matrix in a multidimensional system such as the mammalian skull is frequently hampered by practical limitations imposed by experimental designs, because its accurate estimation demands large sample sizes with known genealogies (Garcia et al. 2014; Steppan et al. 2002). On the other hand, a phenotypic matrix (P-matrix) is easier to obtain and is often accepted as a good proxy of its genetic counterpart, especially for morphological traits (Arnold 1981, 1992; Cheverud 1988, 1995, 1996b; Roff 1995, 1996; Ackermann and Cheverud 2000; Marroig and Cheverud 2001; Goswami 2006a; Kruuk et al. 2008; Porto et al. 2009, 2015; Willmore et al. 2009; Garcia et al. 2014; Puentes et al. 2016; Sodini et al. 2018).

Phenotypic covariance can be estimated at different biological levels (Klingenberg 2014) and for decades has been the focus of significant attention among evolutionary biologists. However, despite this increasing interest in morphological integration, how it evolves on a macroevolutionary scale and its potential causes remain poorly understood, and need to be investigated empirically on a case by case basis (Steppan et al. 2002; Arnold et al. 2008; Haber 2015). Previous large-scale studies within several mammalian orders suggested that integration patterns (i.e., the relationships between morphological elements) are remarkably conserved in most taxa (Cheverud 1996b; Ackermann and Cheverud 2000; Marroig and Cheverud 2001; Goswami 2006b; Oliveira et al. 2009; Porto et al. 2009, 2015; Haber 2015; Hubbe et al. 2016), while magnitudes (i.e., the intensity of association between traits) display significant variation even between closely related species (Oliveira et al. 2009; Porto et al. 2009). Investigations of phenotypic matrix evolution within mammalian orders also highlighted dissimilarity in the integration patterns for species, genera (Oliveira et al. 2009; Shirai and Marroig 2010; Hubbe et al. 2016), and between families (Haber 2015; Machado et al. 2018), thus indicating that the evolution of the covariance structure is still an open question in evolutionary biology and depends on the phylogenetic scope been addressed. The stability of covariation patterns has often been associated with stabilizing selection operating through a common epigenetic developmental system (Cheverud 1996a; Marroig and Cheverud 2001; Ackermann 2002; Mitteroecker and Bookstein 2008; Jamniczky and Hallgrímsson 2009; Roseman et al. 2011). There is also substantial evidence from theoretical, simulation, and experimental studies that suggest that covariation structure does actively evolve (Turelli 1988; Roff 2000; Steppan et al. 2002; Blows and Higgie 2003; Jones et al. 2003, 2004, 2012, p. 201; Jones 2007; Revell 2007; Arnold et al. 2008; Jamniczky and Hallgrímsson 2009; Pavlicev et al. 2011; Pitchers et al. 2013; Melo and Marroig 2015; Assis et al. 2016; Penna et al. 2017). So, if we want to understand the phenotypic diversification seen today, and how species evolve, in terms of trajectory, pace, and rate of evolution, then investigating how variation in multidimensional traits changes through time becomes a key question in biology. Therefore, elucidating the potential factors favoring the covariance structure stability or affecting its evolution remains a fundamental challenge to be addressed in evolutionary biology, and will certainly enhance our understanding of how complex morphologies appear and diversify through time.

We explored the evolution of morphological integration in the most ecologically diverse clade of mammals, the New World leaf-nosed bats, using a large dataset and combining both phylogenetic comparative methods and quantitative genetic approaches. The family Phyllostomidae evolved in the New World in the last 30 million years (Rojas et al. 2016), and living species have been highly successful in exploiting an array of roosting environments (Kunz and Lumsden 2003; Voss et al. 2016; Garbino and Tavares 2018) and food resources (Giannini and Kalko 2004). Their feeding strategies are exceptionally diverse among mammals, including insects, vertebrates, fruit, pollen, nectar, young leaves, and even blood (Ferrarezi and Gimenez 1996; Freeman 2000; Wetterer et al. 2000; Giannini and Kalko 2004; Gardner 2007; Baker et al. 2012). This diversity is reflected in their morphology, and their impressive cranial diversity provides an excellent system for investigating the evolution of complex phenotypes (Nogueira et al. 2009; Monteiro and Nogueira 2010, 2011; Santana et al. 2010, 2012; Dumont et al. 2011, 2014; Pedersen and Müller 2013; Rossoni et al. 2017; Yohe et al. 2017, 2018).

The aim of our study is twofold: (1) to examine the long-term evolution of morphological integration structure in the skulls of a broad sample of phyllostomid bats by comparing the similarity patterns and overall magnitude of integration across species and clades; (2) to investigate the relationships between patterns and magnitudes of integration, dietary strategies, roosting ecology, and morphological differentiation (i.e., the amount of evolution in multivariate traits) during phyllostomid evolution, to understand how the covariance structure evolve. These main goals lead to several questions that will be tested and discussed throughout the Manuscript: Has the cranial covariance structure remained stable over 30 million years of diversification of the New World leaf-nosed bats? If not, where the divergence is concentrated in the phylogeny? Is the evolution of morphological integration associated with dietary specializations and roosting ecology? Has morphological integration changed as a by-product of selection acting on species average morphology? Are the covariance patterns of particular traits associated with diet and roosting?

Materials and Methods

SAMPLES, PHYLOGENY, AND TAXONOMIC FRAMEWORK

We examined 2665 specimens, representing all currently recognized subfamilies, 45 genera, and 48 species of phyllostomid bats located in Brazilian and North American Natural History Museums. Table S1 provides the sample sizes per species analyzed. The phylogenetic estimates were obtained from Rojas et al. (2016) (TreeBase S17602). We followed the subfamily taxonomic classification proposed by Baker et al. (2003, 2012), in which 11 subfamilies, 12 tribes, and 56 genera are recognized.

DATA ACQUISITION, MEASUREMENTS, AND DATA ANALYSIS TOOLS

We recorded three-dimensional coordinates for 21 cranial landmarks (Fig. 1, Table S2) using a Microscribe MX 3D, and from

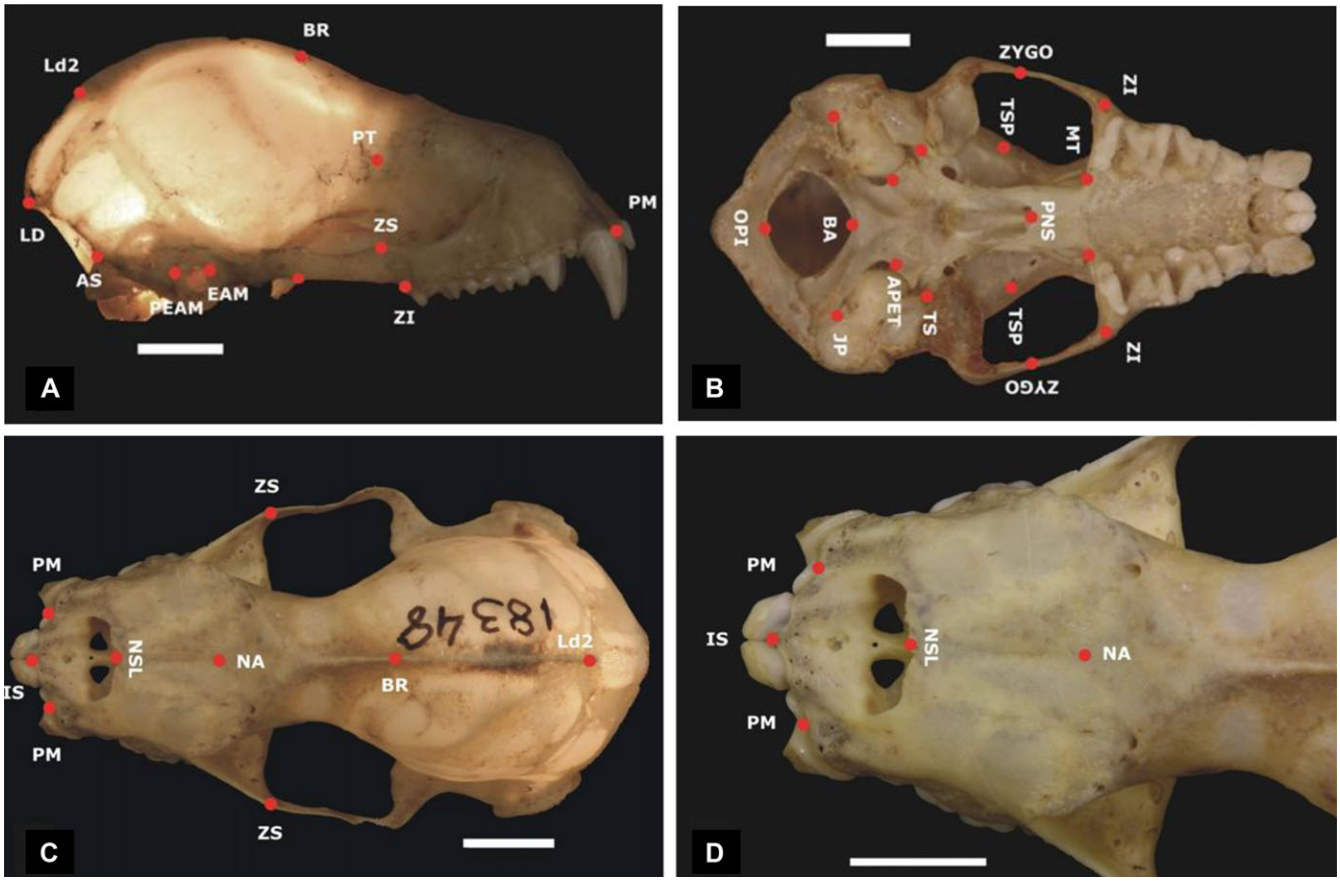

Figure 1. Cranial anatomical landmarks shown on *Chrotopterus auritus* (A–B; MZUSP 3077) and *Phyllostomus hastatus* (C–D; MZUSP 18348). (A) Lateral view. (B) Ventral view. (F) Dorsal view. (G) Dorsal view with nasal and frontal bones in detail. Scale bar = 5 mm. See Tables S2 and S3 for landmarks and linear distances descriptions.

these landmarks, we calculated a set of 35 linear distances describing cranial morphology (Table S3). Landmarks and the derived interlandmark Euclidean distances were first established by Cheverud (1982) and reflect important developmental and functional relationships among cranial elements, while simultaneously representing the overall morphology of the skull (Cheverud 1982; Marroig and Cheverud 2001; Porto et al. 2009). The landmarks are positioned at the intersection between sutures or other discrete and homologous cranial features. Only skulls from adult specimens were measured. Specimens were considered adults when the basisphenoid and basioccipital joint (*synchondroses intersphenoidalis and spheno-occipitalis*) was completely fused. To accurately place the anatomical landmarks on phyllostomid skulls, we used a stereomicroscope, and when intense illumination was required, a 5-mm light source was positioned on the inside of the foramen magnum.

Bilaterally symmetrical measurements were averaged, and if one side of the skull was damaged, measurements taken from the other side were used instead of the average. All specimens were digitized twice and repeatability was estimated to account for measurement error (Lessels and Boag 1987). An exploratory data analysis (Tukey 1977) was performed to check the normality of each distance measurement and to highlight potential outliers. Repeatabilities were high for all species (mean = 0.91; SD = 0.05, Table S4), and no significant deviation from normality was observed. All subsequent analyses were carried out using the averages of repeated measurements using R version 3.5.0 (R Core Team 2018).

ESTIMATION OF INTRAPOPULATIONAL CORRELATION AND COVARIANCE MATRICES

Patterns of within-group phenotypic correlation and covariance matrices (P-matrices) were estimated for each species and will be referred to from now on as correlation and covariance matrices, respectively. We used the phenotypic matrix as a substitute for G-matrix. Studies comparing genetic and phenotypic within-group matrices among populations, species or higher taxa, suggest that P-matrices can be generally accepted as a good proxy of their genetic counterparts, especially for morphological traits (Arnold 1981, 1992; Cheverud 1988, 1995, 1996b; Roff 1995,

1996; Arnold and Phillips 1999; Marroig and Cheverud 2001; Ackermann and Cheverud 2002; Goswami 2006a; Porto et al. 2009, 2015; Marroig and Cheverud 2010; Garcia et al. 2014). Moreover, the similarity between P- and G-matrices has been investigated several times for the same set of traits used in our study, and has been shown to be quite similar in rodents and mammals in general (Cheverud, 1988; Porto et al., 2009, 2015; Marroig & Cheverud, 2010; Garcia et al., 2014; Hubbe et al., 2016), thus validating the "Cheverud Conjecture" (Cheverud 1988).

Geographic variation, sex, and their possible interaction were evaluated through MANOVA, with models chosen on the basis of the Wilk's lambda statistic, with alpha level of significance set at $P = 0.05$ (Table S1). When sources of variation significantly influenced the data, covariance matrices were estimated using the residual matrix of a general linear model, including the 35 distances as dependent variables and significant sources of variation as independent variables. In cases where no effect was detected, the covariance matrices were estimated directly from raw data.

Additionally, for each node of the phylogenetic tree, we calculated the ancestral within-group covariance matrices (W-matrices) using two approaches: (1) pooled within-group matrices along the phylogeny and (2) by maximum likelihood ancestral state reconstruction of each variance and covariance as independent elements (see Supporting Information 1 for a detailed explanation of both methods).

COMPARISONS OF CORRELATION AND COVARIANCE PATTERNS

We quantified the similarity of correlation and covariance matrices between species using the Random Skewers (RS) (Cheverud 1996b; Cheverud and Marroig 2007), Krzanowski (Blows et al. 2004; Krzanowsky 1979), and Riemann distance methods (Mitteroecker and Bookstein 2009). Because these three metrics provided essentially the same results, only those obtained by the RS technique are presented in the main text (see Supplementary Material "*Krzanowski's* method" and "Riemannian distance method" for specific descriptions of these methods and the results obtained using these metrics).

The RS method is based on evolutionary theory and can be fully interpreted within the theoretical framework of quantitative genetics (Hansen and Houle 2008; Lande 1979), providing information on how similar populations would respond on average to selection. This procedure is a direct application of the multivariate response to selection equation ($\boldsymbol{\Delta z} = \mathbf{G}\boldsymbol{\beta}$), and involves multiplying each matrix (here $\mathbf{P}$ as a substitute for $\mathbf{G}$) by random selection vectors ($\boldsymbol{\beta}$) and comparing the response vectors ($\boldsymbol{\Delta z}$) between each pair of matrices for the same simulated multivariate selection vector (see also Hansen and Houle 2008). The cosine of the angle formed between any two vectors is a measure of their correlation. The response vectors are then correlated and the average across a large number of vectors is used as a measure of the similarity between compared matrices (Cheverud and Marroig 2007; Oliveira et al. 2009). In this study, we compared the evolutionary responses of each pair of matrices to 10,000 randomly generated selection vectors obtained from a multivariate normal distribution and normalized to a length of one. Because the same random selection vector was applied to both matrices, any differences in the orientation of the responses would be due to differences in the matrices being compared. This analysis provides a measure of association, or in other words, a measure of the degree of similarity among structural patterns of correlation and covariance matrices. The statistical significance of this vector is determined by the distribution of correlations among random vectors. If two matrices have the same or very similar covariance patterns, the average response to random selection vectors is expected to be colinear ($r \sim 1.0$). Otherwise, if they lack a common structure, the average response is expected to be perpendicular or equal to zero ($r = 0.0$). If they are mirror images of each other with opposite signs, the correlation should approach –1.0. Explicitly, the significance test performed here considers the null model (absence of shared structure, i.e., no similarity) among the phenotypic correlation and covariance matrices of phyllostomid bats. If the average observed correlation vector between two matrices exceeds 95% correlation between random vectors, it is assumed that a significant structural similarity exists between the two matrices. Perhaps more important than the significance per se is the observed degree of matrix similarity, because this quality is at the core of quantitative genetics' evolutionary applications (Haber 2015; Marroig and Cheverud 2001).

Finally, sample size can affect estimations of individual matrix elements due to sampling error (Cheverud 1996b; Marroig and Cheverud 2001; Porto et al. 2009). Thus, we assessed matrix repeatability to evaluate the level of similarity. Correlation and covariance matrix repeatability was calculated using a Monte Carlo approach, in which 10,000 bootstrap resamplings of the original data were made with a constant sample size after removing other sources of variation (as described above and in Table S1). These matrices were calculated for each of the resamples and compared to the original matrix using the RS method, and the average vector correlation was then used as a measure of repeatability. To evaluate how robust our dataset is with respect to sampling, we performed a rarefaction analysis using the species with the largest number of sampled individuals in our dataset (see Supplementary Material "Rarefaction Analyses"). Based on the results of RS, we produced a pairwise similarity matrix between species that corresponds to the integration patterns similarity matrix.

MATRIX CORRELATION

Analyzing the relationship among morphological integration (patterns and magnitudes), phylogeny, morphology, diet, and roosting

We used matrix correlations to investigate the relationships between matrices that quantify the dissimilarity among morphological integration (patterns and magnitudes), phylogeny, morphology, diet, and roosting. For that, the integration patterns similarity matrix (Table S5), obtained by RS approach, was converted into a Euclidean distance matrix using:

$$\mathbf{D}_{hi} = \sqrt{2(1 - \mathbf{S}_{hi})}, \quad (1)$$

where **D** is the distance matrix and **S** is the similarity matrix (Haber 2015).

We used the average coefficient of determination (r^2) to calculate the integration magnitude, by averaging the squared correlations in correlation matrices (Cheverud 1988; Cheverud et al. 1989; Oliveira et al. 2009; Pavlicev et al. 2009; Porto et al. 2009, 2013; Shirai and Marroig 2010). Then, we estimated the Euclidean distance matrix between species r^2 values (*r2Dis*; Table S6). To statistically investigate differences in r^2 between phyllostomid species, we bootstrapped the data for each species, calculating the correlation matrices and r^2 for each of the 10,000 resamplings with replacement.

We produced a phylogenetic distance matrix (Table S7) between all species analyzed using the function cophenetic.phylo from the R package *ape* (Paradis et al. 2004). We also estimated the Mahalanobis (D^2) distance between species (Table S8) as a measure of multivariate morphological divergence (Ackermann 2002) using the following equation:

$$D^2_{ij} = (\mu_{i-}\mu_{j})\mathbf{W}^{-1}(\mu_{i-}\mu_{j}), \quad (2)$$

where μ_i and μ_j are the vector of means for the i^{th} and j^{th} population, respectively, and **W** is the ancestral pooled within-group covariance matrix. This equation was implemented in the R package *evolqg* (Melo et al. 2015) using the MultiMahalanobis function. The morphological distance matrix was then used to investigate the relationship between species multivariate average phenotype and morphological integration patterns (Marroig and Cheverud 2001; Ackermann 2002; Oliveira et al. 2009), as integration patterns might have changed as a by-product of changes in species average morphology. This measurement represents the amount of evolution in trait averages and will be described hereafter as morphological differentiation.

Additionally, we constructed ecological matrices based on diet (Table S9) and roosting ecology (Table S10) similarities among phyllostomid species. Species diets were quantified as the proportions of a species' diet constituted by five different feeding strategies: insectivory, carnivory, hematophagy, nectarivory, and frugivory. A pairwise dietary similarity matrix was calculated as the sum across the five categories, where each category had a value corresponding to the square root of the product of paired species-specific values in the same category, as follows:

$$\begin{aligned}\text{Dietary similarity}_{(sp1,sp2)} = {} & \sqrt{(\%I_{sp1} \times \%I_{sp2})} \\ & + \sqrt{(\%C_{sp1} \times \%C_{sp2})} + \sqrt{(\%H_{sp1} \times \%H_{sp2})} \\ & + \sqrt{(\%N_{sp1} \times \%N_{sp2})} + \sqrt{(\%F_{sp1} \times \%F_{sp2})}, \quad (3)\end{aligned}$$

where I, C, H, N, and F represent insectivory, carnivory, hematophagy, nectarivory and frugivory, respectively. The same method was used for roosting ecology using three categories: cave, cavity, and foliage. Dietary and roosting information was obtained from the previous literatures (Nowak and Walker 1994; Ferrarezi and Gimenez 1996; Freeman 2000; Wetterer et al. 2000; Kunz and Lumsden 2003; Giannini and Kalko 2004; Simmons 2005; Rodríguez-H. et al. 2007; Gardner 2008; Datzmann et al. 2010; Baker et al. 2012; Voss et al. 2016; Garbino and Tavares 2018) and supplemented by personal experience (N. P. Giannini).

As done for the integration patterns similarity matrix, the dietary and roosting similarity matrices were transformed into Euclidean distance matrices based on Haber (2015) (Equation (1) above). From now on, we will adopt the following terms and abbreviations for each of these Euclidean distance matrices: (a) Covariance distance matrix also known as integration patterns (*RSDis*); (b) r^2 distance matrix also known as integration magnitudes (*r2Dis*); (c) Phylogenetic distance matrix (*PhyloDis*); (d) Morphological distance matrix (*MorphDis*); (e) Dietary distance matrix (*DietDis*); and (f) Roost distance matrix (*RoostDis*).

Comparisons between these variables were performed using matrix correlation, and the significance was obtained through permutation tests (Mantel 1967). We also calculated matrix partial correlations conditioning the variation of *RSDis*, *r2Dis, MorphDis*, *DietDis*, and, *RoostDis* on the phylogenetic distance matrix between species (*PhyloDis*) (Dow and Cheverud 1985; Marroig and Cheverud 2001) using the phylogenetic permutation procedure proposed by Harmon and Glor (2010).

RELATIONSHIPS BETWEEN FEEDING STRATEGY AND ROOSTING ECOLOGY AND COVARIANCE PATTERNS OF INDIVIDUAL TRAITS

We used the Selection Response Decomposition method (SRD; Marroig et al. 2011) to investigate whether different dietary strategies and roosting ecologies influenced similarities in covariance patterns of particular traits in phyllostomid bats. Given the functional and biomechanical requirements imposed by dietary and roosting strategies, we predict that those covariance

patterns of traits related with the rostrum/palate extension and retraction, muscle mechanics, and biting performance will show significant correlation with diet and roosting matrices. The SRD is an extension of the RS method, but instead of comparing all of the evolutionary response vectors ($\Delta\mathbf{z}$) between matrices, the $\Delta\mathbf{z}$ component is broken down into its two subcomponents: those due to direct selection acting on a trait, and those due to correlated selection (i.e., a response acting on a given trait due to its covariance with other traits under selection). Although the RS method provides an overall measure of the similarity between any two matrices, the SRD highlights which traits diverged more and/or remained particularly similar in their covariance between morphologies. We compared these trait-specific response vectors between each pair of matrices using vector correlations. The average correlation among these vectors was obtained by repeating the process for each of the 10,000 random selection vectors, and is referred to as the SRD score. To explore whether the dietary distance matrix (*DietDis*) and roosting distance matrix (*RoostDis*) are related to patterns of morphological integration associated with each individual trait, we generated 35 matrices (one for each Euclidean distance) using the SRD score, and compared each with *DietDis* and *RoostDis* using matrix correlation. The significance was assessed via permutation test (Mantel 1967). The SRD analysis was performed using the corresponding function in the R package *evolqg* (Melo et al. 2015).

PHYLOGENETIC COMPARATIVE ANALYSIS

Phylogenetic decomposition analysis of morphological integration patterns and magnitudes

We used the diversity decomposition analysis (decdiv, Pavoine et al. 2010) to investigate the disparities of the integration patterns and magnitudes in a phylogenetic context (see also Haber 2015 and Machado et al. 2018). The method allows testing whether the divergence is (1) concentrated on a single node; (2) concentrated on a few nodes; and (3) concentrated toward the root or the tips of the tree. This test consists of decomposing the distances matrices (*RSDis* and *r2Dis* in our case) along the phylogenetic tree and estimating the contribution of each node to the overall character distribution, testing the null hypothesis of a random structure (see also Haber 2015 and Machado et al. 2018). Significance was carried out using 999 permutations of the tip labels of the phylogeny.

Trait evolution models

We used Brownian Motion (BM) and Ornstein–Uhlenbeck (OU) models of trait evolution to test whether changes in feeding habits might have led to changes in cranial integration patterns, magnitudes, and morphological differentiation among phyllostomid clades. For that, we performed a principal coordinate analysis (Pcoord or PCoA) in *RSDis*, *r2Dis*, and *MorphDis* and used the first two eigenvectors in the subsequent analysis implemented in R package *mvMORPH* (Clavel et al. 2015; R Core Team 2018). We established multiple hypotheses for the evolution of varied feeding habits, each gradually increasing in complexity. The first model included three feeding regimes (Diet OUM.3): (1) obligate frugivores (short-faced bats); (2) frugivores, hematophagous, and generalists; and (3) nectarivores. The next model corresponded to four adaptive peaks (Diet OUM.4) and included: (1) obligate frugivores; (2) frugivores and generalists; (3) nectarivores; and (4) hematophagous bats. Diet OUM.5 discriminated among: (1) obligate frugivores; (2) frugivores; (3) nectarivores; (4) animalivores; and (5) hematophagous. Diet OUM.7 discriminated among: (1) obligate frugivores; (2) frugivores; (3) nectarivores; (4) omnivores; (5) carnivores; (6) insectivores; and (7) hematophagous. Finally, Diet OUM.8 included the strict insectivores to the previous model. Model BM1 assumes that there is no difference between the feeding specializations and that integration magnitude evolves according to BM, accounting for unique rates of evolution in each trait. Model BMM allows variables (integration patterns, magnitudes, and morphological differentiation) to evolve at varying rates in different feeding classes. Model OU1 accounts for the hypothesis of single peak stabilizing selection, in which there is a unique selective regime for the whole phylogenetic tree and the variables under study evolve to the same optimum (i.e., a single optimum for all species). Contrastingly, model OUM allows for multiple selective regimes, or separate optima with single phenotypic rate and single strength of selection between feeding categories. If dietary habits and roosting ecologies do influence the tempo and/or the mode of integration patterns, magnitudes, and morphological differentiation, then we would expect either the BMM or OUM model to best fit our data. Conversely, if dietary habits and roosting ecologies have no influence on the focal variables, then we would expect the other models to be a better fit. Finally, the model EB was used to explore the hypothesis of an early-burst model of trait evolution, in which evolutionary rates decrease over time (Harmon et al. 2010; Slater and Pennell 2014).

Model hypotheses applied to roosting ecologies also followed a trend of gradual complexity, distinguishing first the foliage species from the others (Roosting OUM.2), then treating cave, cavity, and foliage as separate categories (Roosting OUM.3), and finally treating foliage, cavity, cave, cavity-cave (which means predominantly cavity and secondarily cave), and cave-cavity (which means predominantly cave and secondarily cavity) as separate classes (Roosting OUM.5). We used Akaike's information criterion (AIC) along with estimates of ΔAICc and AICc weights, to determine the relative support of each model. The details of additional analysis to test for model adequacy are described in the Supporting Information 2.

Disparity through time

To examine the patterns and magnitudes of integration during phyllostomid diversification over time, we produced relative disparity through time (DTT) plots (Harmon et al. 2003). This method estimates the mean phenotypic disparity within clades in a phylogeny, dividing that by the disparity of the entire group (or to the between-clade disparity). The empirical DTT curve is compared to a distribution of 10,000 simulated curves generated under a BM evolutionary model using the morphological disparity index (MDI; Slater et al. 2010, 2017). The MDI measures the amount of space between the line of the empirical curve and the median of the simulated curves. When the curve for the empirical data lies above the median for the simulated data (positive MDI), the disparity within clades is higher than expected under BM, relative to the between-clade disparity. In this case, trait evolution deviates from BM in the direction of a single, stable adaptive zone (stabilizing selection) or follows a "Late Burst" model (Edwards et al. 2015). Negative MDI values indicate that the empirical curve lies below the simulated lines, suggesting that disparity between clades is higher than expected under BM, relative to disparity within clades. In this case, trait evolution deviates from BM in a way similar to an "Early Burst" consistent with an adaptive radiation model. Here, we adapted the original *dtt* function in R package *geiger* (Harmon et al. 2008) to allow analysis of multivariate pairwise distance matrices (*RSDis* and *r2Dis*). R codes are provided as Supporting Information.

Results

COMPARISONS OF CORRELATION AND COVARIANCE PATTERNS

The first question addressed in our study was whether the phenotypic covariance and correlation patterns were similar across phyllostomid lineages. All results from RS analyses were significantly different than zero ($P < 0.0001$) both between species (Fig. 2 and Table S5) and across the entire phylogenetic tree (Tables S11 and S12), suggesting that, on a broader scale, the family Phyllostomidae share similar patterns of cranial morphological integration. With some exceptions, within-clade species comparisons presented a higher similarity in morphological integration patterns (Figs. S1–S5). In addition to the overall similarity, our results also revealed divergences in morphological integration patterns, especially from comparisons between species belonging to distant phylogenetic clades (Fig. 2 and Table S11). The lowest similarities among species were found in comparisons between *Choeronycteris mexicana* (Subfamily Glossophaginae; nectarivore) and *Centurio senex* (Subtribe Stenodermatina; obligate frugivore) (0.42 raw and 0.44 adjusted; Table S5 and Fig. 2). Figure S6 represents the average similarity of integration patterns for 48 species grouped by feeding specializations, based on comparisons of covariance matrices using RS method. Note that some nectarivorous and obligate frugivorous species presented the lowest values in the boxplot. RS results obtained from the most important clades of the phyllostomid phylogeny are presented in Figures S1–S5 and Tables S11 and S12. Raw and adjusted RS values were highly correlated for both correlation and covariance matrices (Pearson's $r = 0.988$, $P < 0.001$ and Pearson's $r = 0.990$, $P < 0.001$, respectively). The mean pairwise adjusted similarity patterns were broadly equal when calculated by covariance or by correlation matrices (Fig. S7). The lower raw and adjusted similarities for correlation and covariance matrices compared were associated with lower sample sizes (Fig. S8). See Supplementary Material "Rarefaction Analyses" for further discussion on sample reliability (Fig. S9). We have removed the first principal component from the phenotypic covariance matrices and evaluated the similarity between species using RS procedure. Ours results showed that the similarity decreased 0.10 on average (minimum 0.02 and maximum 0.23) when comparing the original matrices and the matrices with the allometric component removed. Although it does not have a significant impact on the similarity, allometric size variation is an important component maintaining the morphological integration structure.

Additionally, for visualization purposes, we projected the first two PCoA axes obtained from the *RSDis* to represent the distribution of taxa in the morphological integration patterns space (Fig. 3). The first two axes explain, respectively, 12.33% and 11.21%, of the total variation. The distribution shows a grouping of species in their respective subfamilies with some overlap between them (Fig. 3). On both PCoA axes, the nectarivorous (Subfamily Glossophaginae) and strict insectivorous (Subfamily Lonchorhininae) clades showed no overlap with other families, with the former presenting lowest values in the represented axes (Fig. 3). Little overlap was found in the clade representing obligate frugivores and hematophagous species (Subtribe Stenodermatina and Subfamily Desmodontinae, respectively, Fig. 3).

INTEGRATION MAGNITUDES

The overall magnitude of integration among traits, measured by r^2, varied across species from 0.046 (*Sphaeronycteris toxophyllum*) to 0.15 (*Micronycteris microtis*), with an average of 0.08 (Fig. S10). The inferred evolution of integration magnitude can be visualized in a "traitgram" (Fig. S11, function phenogram in package "phytools" for R; Revell 2012). This figure represents a projection of the phyllostomid phylogenetic tree into a space defined by the integration magnitude (r^2 values) and time since the root (Myr) (see Evans et al. 2009; Revell 2012).

MATRIX CORRELATION

Our second goal consisted of analyzing the relationships between patterns (*RSDis*) and magnitudes (*r2Dis*) of integration, dietary

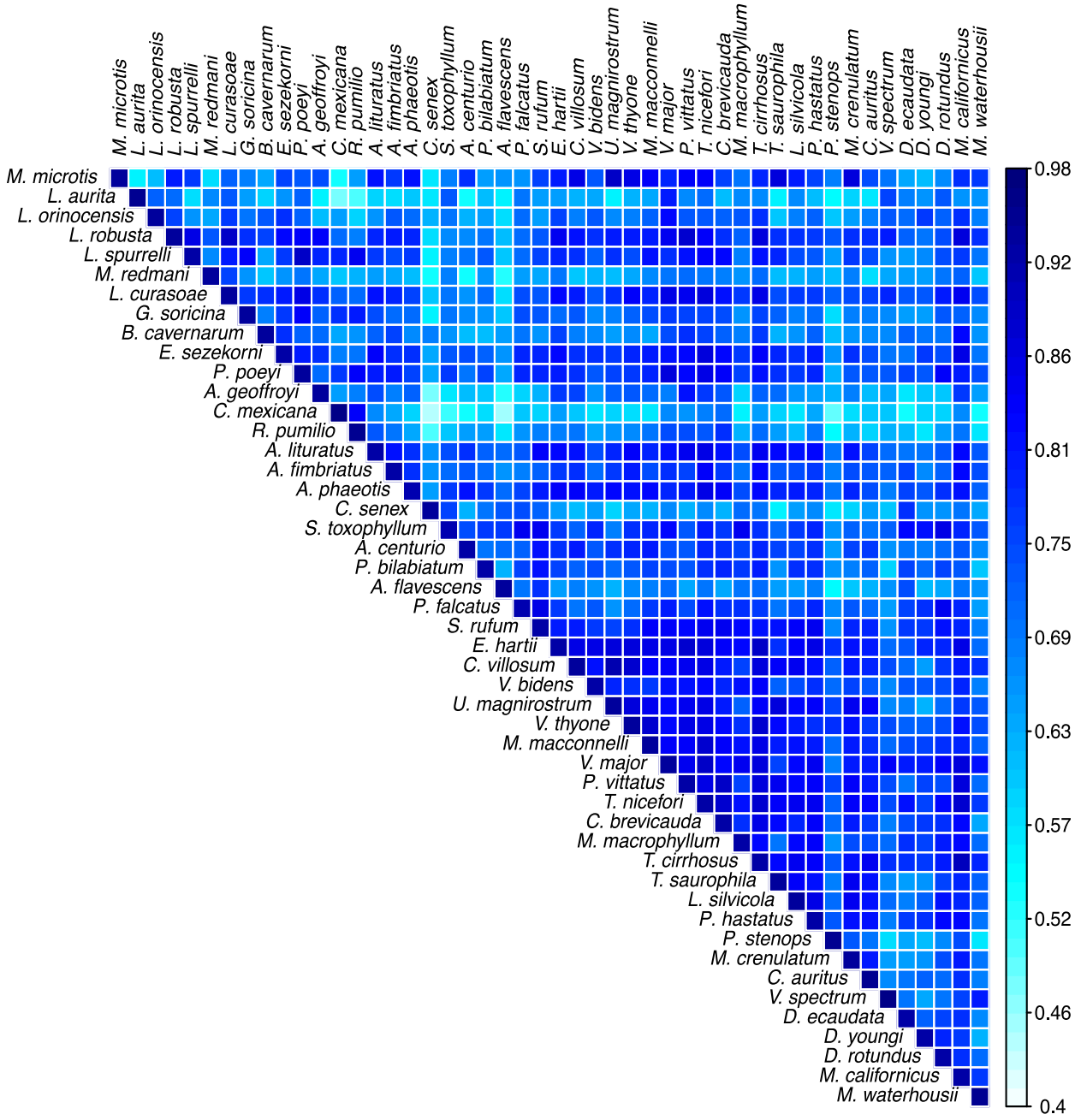

Figure 2. Average vector correlations between covariance matrices responses to 10,000 random selection vectors for each pairwise species comparisons (matrix similarity—Random Skewers). The diagonal contains the matrix repeatability for each species.

strategies (*DietDis*), roosting ecology (*RoostDis*), and morphological differentiation (*MorphDis*). Results from standard and partial correlations between species average morphologies (*MorphDis*) and morphological integration patterns (*RSDis*) were significant for both covariance and correlation matrices (Table 1). Our analysis also indicated a significant association between ecological variables (*DietDis* and *RoostDis*) and *RSDis* in the standard correlation test (Table 1). However, this result was no longer significant when phylogenetic relatedness was taken into account (Table 1), suggesting that these variables are phylogenetically structured. Matrix correlation results among *MorphDis*, *DietDis*, and, *RoostDis* are provided in Table 2.

RELATIONSHIPS BETWEEN FEEDING STRATEGIES AND INDIVIDUAL TRAIT COVARIANCE PATTERNS

SRD results revealed that dietary strategies and roosting ecology of phyllostomid bats influenced patterns of morphological integration in cranial traits. Six cranial traits associated with

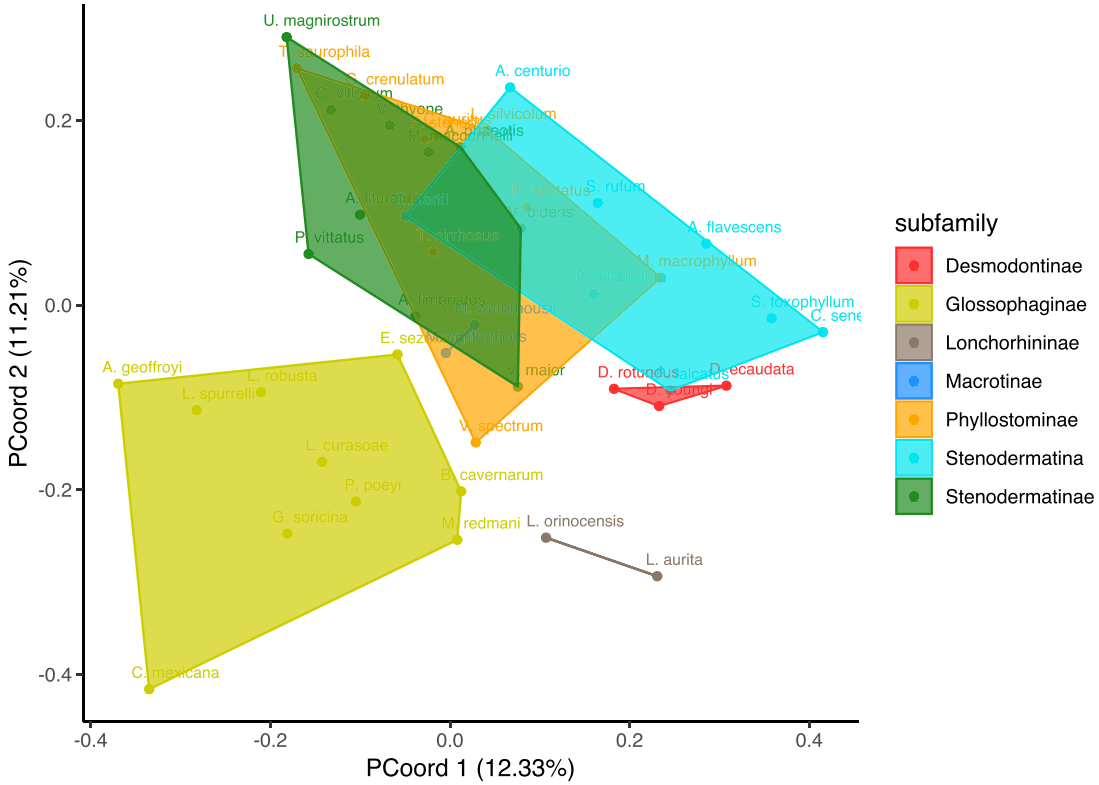

Figure 3. Principal coordinate analysis (PCoord) of *RSDis* showing the position of species and Subfamilies in the integration space defined by two PCoA axes. Colors presented here match those of the Figure 5.

Table 1. Standard and partial matrix correlations between dissimilarity matrices of integration patterns (covariance and correlation matrices with raw and adjusted values), and dietary, roosting, morphological, and r2 distances among phyllostomid species.

	Random Skewers observed		Random Skewers adjusted	
	Covariance	Correlation	Covariance	Correlation
Matrices	Standard matrix correlations			
Diet (*DietDis*)	**0.166**	**0.175**	**0.174**	**0.174**
Roosting (*RoostDis*)	**0.084**	**0.112**	**0.086**	**0.118**
Morphological (*MorphDis*)	**0.360**	**0.375**	**0.360**	**0.375**
r^2 (*r2Dis*)	0.124	0.150	0.142	**0.181**
	Partial matrix correlations			
Diet (*DietDis*)	0.109	0.108	0.105	0.09
Roosting (*RoostDis*)	0.02	0.04	0.01	0.05
Morphological (*MorphDis*)	**0.346**	**0.360**	**0.345**	**0.358**
r^2 (*r2Dis*)	0.106	0.130	0.123	0.161

Note: Partial correlations were estimated by conditioning the association of pairwise correlations on a matrix of phylogenetic distance. Boldface values indicate significant results at $P < 0.05$.

the face and two associated with neurocranial regions were significantly correlated with the dietary matrix (Table S13). Those associated with the face region were related to the oral (PM–ZI and MT–PNS), nasal (NSL–NA and NA–PNS), and zygomatic regions (ZYGO–TSP), as well as one trait spanning both the oral and nasal subregions (NSL–ZI) (Table S13, Fig. 4). Traits associated with the neurocranial region were related to both the vault (BR - APET) and base subregions (APET - TS) (Table S13, Fig. 4). Four cranial traits associated with the face and four associated with the neurocranium were significantly correlated with the roosting matrix (Table S14). Those associated with the face region were related to the oral (MT–PNS), nasal

Table 2. Matrix correlations between morphological, dietary and roosting distances among phyllostomid species.

Matrices	Diet	Roosting	Morphological
Diet (*DietDis*)	1		
Roosting (*RoostDis*)	**0.59**	1	
Morphological (*MorphDis*)	**0.32**	**0.16**	1

Note: Boldface values indicate significant results at $P < 0.05$.

(NSL–NA, and NA–PNS), and zygomatic subregions (ZI–TSP) (Table S14). Those traits associated with the neurocranial region were related to the vault subregion (NA–BR, BR–PT, BR–APET, and BR–LD) (Table S14).

PHYLOGENETIC COMPARATIVE ANALYSIS

Phylogenetic decomposition analysis of morphological integration patterns and magnitudes

The results obtained from the diversity decomposition analysis indicated that the divergence observed for integration patterns and magnitudes are not randomly distributed along the phylogenetic tree (Fig. 5). The null hypothesis of structural randomness was rejected for all tests (Table 3), suggesting a "close-to-root" model in which most of the diversification is significantly concentrated on one or a few nodes close to the root of the phylogeny (Pavoine et al. 2010). The "close-to-root" model corresponds to the classical models of phylogenetic signal in the trait states of extant species, in which closely related species are expected to be more similar to one another and distantly related species are expected to be more dissimilar than would be predicted under a BM (Pavoine et al. 2010). Most of the phylogenetic structure in the integration space (patterns and magnitudes) can be explained by splits at the beginning of the diversification of major clades in the Phyllostomidae.

TRAIT EVOLUTION MODELS

We used models of trait evolution to investigate whether differences in cranial integration patterns, magnitudes, and average morphology may be explained by the varied dietary specializations and roosting behaviors of phyllostomid bats.

The relative support for the explored models of trait evolution based on dietary specializations is shown in the Supporting

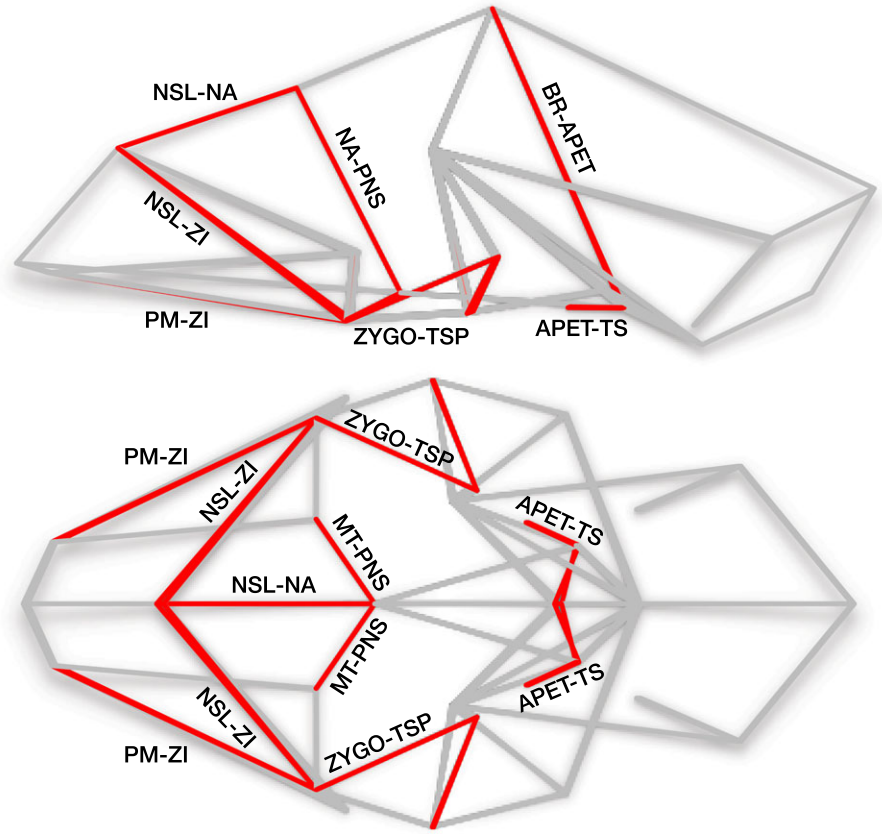

Figure 4. Graphical representation of Selection Response Decomposition (SRD) analysis of each linear distance with diet, drawn on representations of *Ectophyla alba* skull (dorsal and lateral view). Red lines indicate statistically significant results between traits and diet. Six cranial traits associated with the face and two with the neurocranium regions showed significant correlation with the dietary matrix.

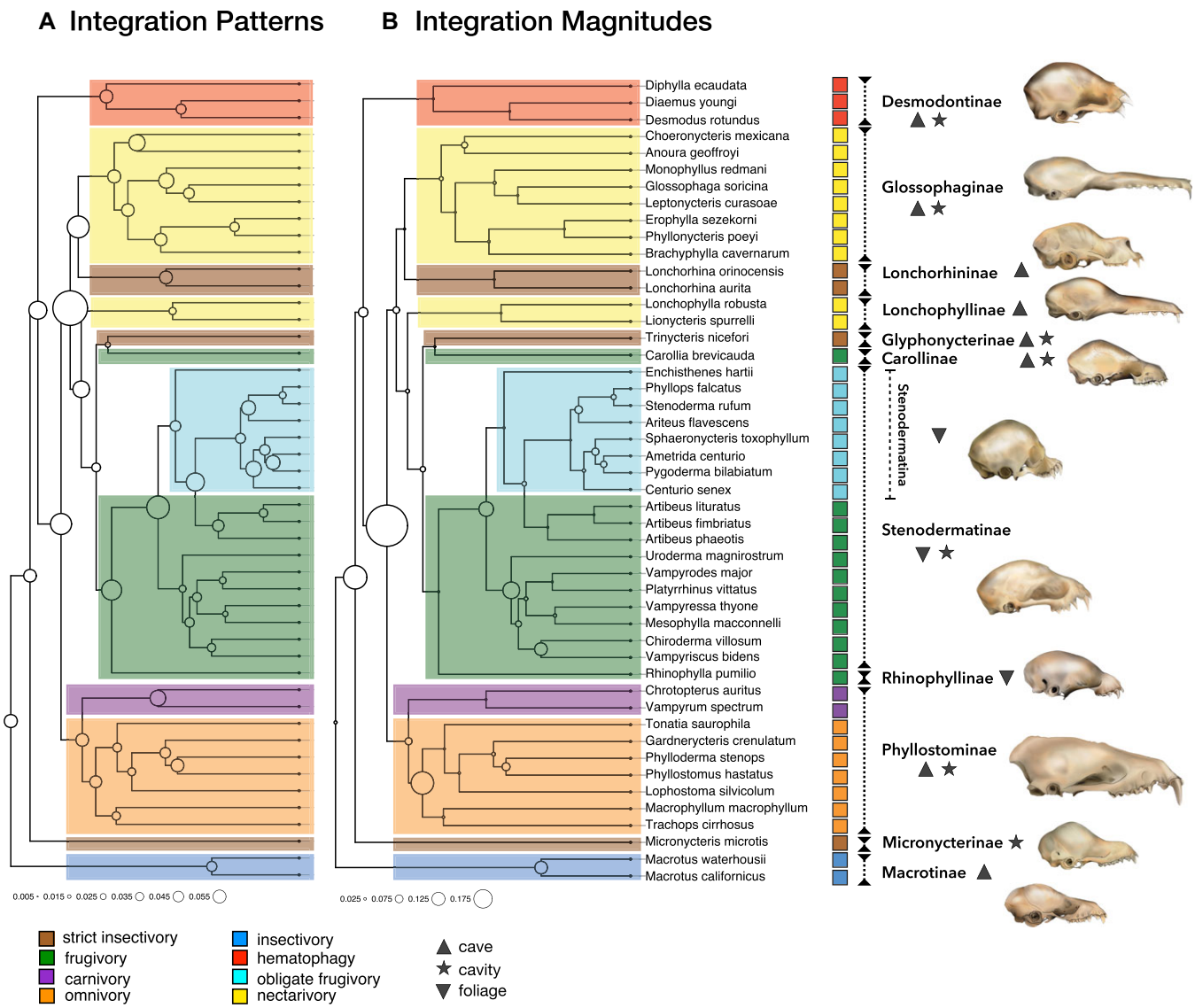

Figure 5. Diversity decomposition analysis for integration patterns (A) and magnitudes (B). The phylogeny was adapted from Rojas et al. (2016) to include all studied species. The size of the circle represents the contribution of each node to the overall character distribution. Labels represent dietary strategies and roosting ecology.

Table 3. Statistics for phylogenetic decomposition analysis (decdiv, Pavoine et al. 2010) of morphological integration patterns and magnitudes.

Variables	Test	Obs	Std.Obs	Alter	*P* value
Integration patterns (RS)	Single nodes	0.0667	7.8429	Greater	0.001
	Few nodes	0.1568	3.3267	Greater	0.001
	Skewed to the root*	0.5753	5.8222	Two sided	0.001
	Skewed to the root**	0.4579	–3.8692	Two sided	0.001
Integration magnitude	Single nodes	0.1525	3.6774	Greater	0.009
	Few nodes	0.4221	3.4250	Greater	0.001
	Skewed to the root*	0.6423	3.5836	Two sided	0.001
	Skewed to the root**	0.4126	–2.6223	Two sided	0.016

*ranking is based on tree topology; **ranking is based on branch lengths.
Obs = observed; Std.Obs = standard deviations of observed values.

Information 2, Figure SI2-1, and Table SI2-1. For cranial integration patterns, we found relative strong support for multi-OU model (best relative supports: OUM.8, 60%; OUM.4, 26%; and OUM.5, 12%, Fig. SI2-1A and Table SI2-1). Likewise, the best relative support found for species average morphology was also a multi-OU models with 61% suggesting seven adaptive peaks (OUM.7) and 26% suggesting eight (OUM.8) (Fig. SI2-1C and Table SI2-1). These results indicated that the evolution of both integration patterns and morphological differentiation had multiple optima corresponding to species occupying different adaptive zones. The BM model with four different rates presented the best relative support for cranial integration magnitudes (BMM.4, 79%; Fig. SI2-1B and Table SI2-1). For this model, the sigma parameter, representing the intensity of stochastic fluctuations in the evolutionary process or the phenotypic rate, was higher for obligate frugivores, suggesting that these species might be evolving under a distinct and possibly less constrained selective regime regarding the magnitude of integration (Fig. SI2-3).

The relative support for the explored models of trait evolution based on roosting ecology is shown in Figure SI2-2 and Table SI2-2. For integration patterns, relative strong support for multi-OU models was found among the 300 replicates of stochastic character mapping histories reconstructed on the mcc tree (OUM.3, 69%; OUM.5, 18%; Fig. SI2-2A and Table SI2-2). For cranial integration magnitudes, we found a relative strong support for a five multi-OU model (OUM.5), favored across OUM.3 (26%) (Fig. SI2-2B and Table SI2-2). The BM model with three different rates (BMM.3, 84%) presented the best relative support in our analysis for average morphology, followed by BMM.5 (16%) (Fig. SI2-2C and Table SI2-2). Parameter estimates under BMM.3 suggested that cavity roosting shows higher phenotypic rate, followed by foliage and cave categories (Fig. SI2-4).

DISPARITY THROUGH TIME

Relative disparities through time plots were produced to examine the time course of patterns and magnitudes of integration during phyllostomid diversification. We found that MDI values were positive and significantly different from simulated curves generated under a BM model of evolution (MDI $RSDis = 0.43$; $P = 0.02$ and MDI $r2Dis = 0.32$; $P = 0.02$; Fig. 6). The evolution of integration patterns was more stable behavior through time, with almost constant average disparities, which always lay above the simulated curves (Fig. 6A). This pattern of divergence is usually interpreted as a product of stabilizing selection (evolution in the direction of a single peak—OU model; stable adaptive zone) or a "Late Burst" model. Comparatively, magnitudes showed remarkable variation over time (Fig. 6B). Despite an overall increase in subclade magnitude disparity over time (MDI $r2Dis = 0.32$; $P = 0.02$), at least three important decreases were observed: one occurring at the beginning of diversification (~27–23 Myr; 0.1 relative time), another coincident with the radiation of several clades and evolution into different dietary adaptive zones (~24–20 Myr; 0.2 relative time), and finally, another decrease ~9 Myr (0.7 relative time) coincident with the radiation of the short-faced bats, subtribe Stenodermatina (Fig. 6B).

Discussion

HAS THE CRANIAL COVARIANCE STRUCTURE REMAINED STABLE OVER 30 MILLION YEARS OF DIVERSIFICATION?

We explored the evolution of cranial covariance structure in a comprehensive sample of phyllostomid bats by phylogenetically analyzing the associations among dietary strategy, roosting ecology, and average morphological differentiation. The first goal of our study was to investigate whether morphological integration remained similar during the diversification of Phyllostomidae. Results of matrix comparisons revealed that phenotypic covariance structure remained relatively conserved on a broad phylogenetic scale, suggesting that New World leaf-nosed bats share an overall pattern of similarity in their cranial morphological integration (Fig. 2, Tables S5 and S11). This stability in the morphological integration structure throughout the evolution of this group was also supported by the high subclade average disparity revealed by DTT analyses (Fig. 6A and B). This result is quite interesting considering the substantial evolutionary timescales of diversification and the myriad of morphological, physiological, and ecological changes associated with feeding specializations in theses bats, and might suggest the relative role of internal constraints in shaping the covariance structure (see Cheverud 1982). With few exceptions, most of the intraclade comparisons between within-species covariance matrices presented higher similarity results. Nevertheless, despite the overall similarity, our analyses also revealed substantial divergence in the morphological integration patterns between interclade comparisons, suggesting that the evolution of the morphological integration in phyllostomid bats depends on the phylogenetic scope been addressed. Although the projection of the only two axes of the Pcoord analyses (Fig. 3) do not explain all the variance in integration patterns, they do show structuring of part of the variation existing in the data, enlighten our understanding of which groups of taxa differ the most in their integration patterns. The most striking feature of this integration space is the absence of overlap (nectarivorous, Subfamily Glossophaginae and strict insectivorous, Subfamily Lonchorhininae) or little overlap (obligate frugivores, Subtribe Stenodermatina and hematophagous species, Subfamily Desmodontinae) of the integration patterns between distant phylogenetic clades. These findings are in agreement with the results of diversity decomposition analysis (Pavoine et al. 2010) discussed below.

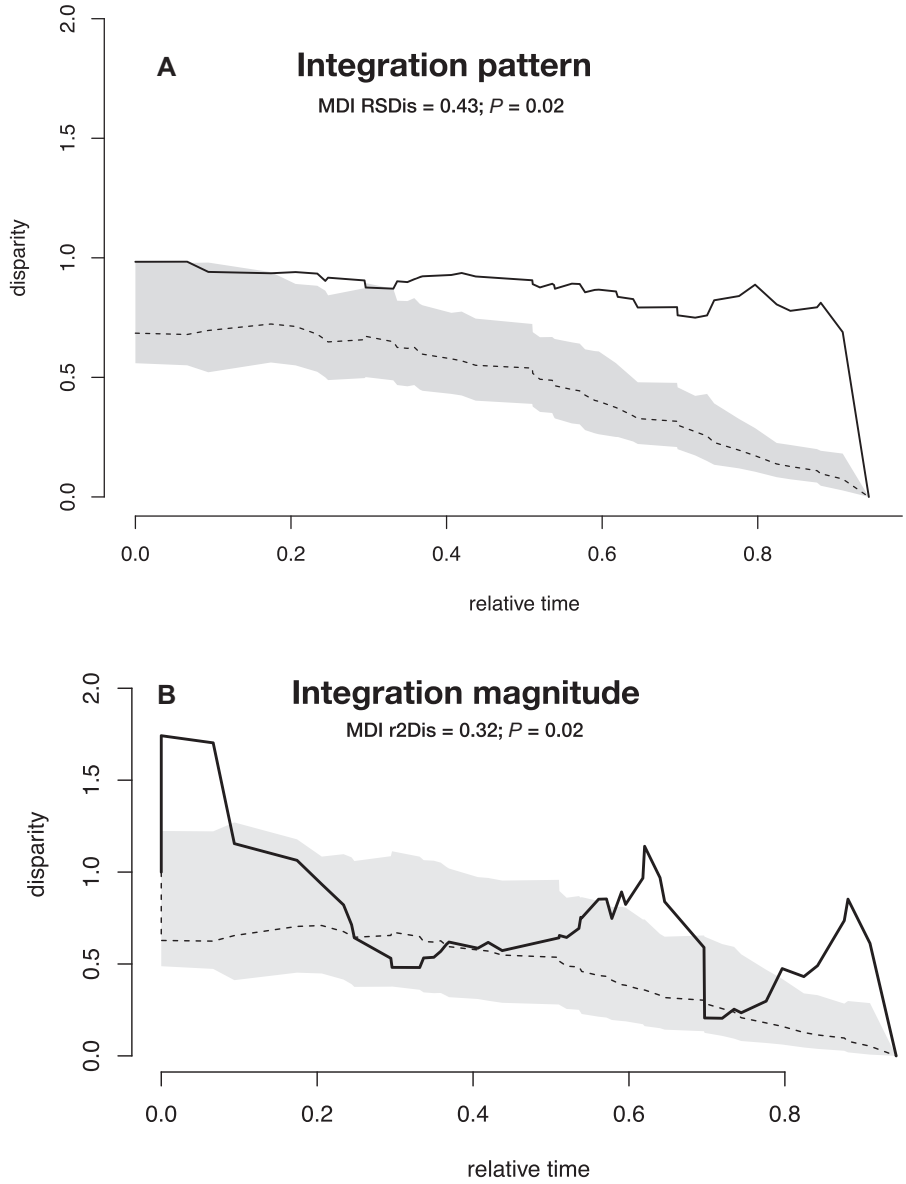

Figure 6. **Relative disparity through time (DTT) plots for integration pattern (A) and integration magnitude (B). Solid line represents the empirical curve. The dashed line represents the median subclade DTT based on 10,000 simulations of trait evolution on the phyllostomid phylogeny under Brownian motion. The grey shaded area indicates the 95% confidence intervals for the null hypothesis of neutral evolution (DTT range for the simulated data). Time shown is relative from the root of the phylogenetic tree to the present.**

PARTICULARS OF DIVERGENCE BETWEEN INTRA- AND INTERCLADE COVARIANCE PATTERNS COMPARISONS

Despite the greater similarities found from intraclade comparisons, some exceptions deserve a case-by-case interpretation. For instance, pairwise comparisons including the nectarivorous species of the Subfamily Glossophaginae, the Antillean bats *Brachyphylla cavernarum*, and *Monophyllus redmani* exhibited the smallest similarities in their patterns of phenotypic covariation (Fig. S2). In a nectarivorous ecomorphological space, *Brachyphylla* represents a plant-visiting generalist species (its diet includes fruits, pollen, nectar, and insects) with relatively short rostra and an unspecialized tongue, being reported as phenotypically similar to frugivorous phyllostomids (Griffiths 1985; Freeman 1995, 1998, 2000; Rodriguez and Dávalos 2008; Datzmann et al. 2010; Monteiro and Nogueira 2011). Conversely, *Monophyllus* possesses an elongated muzzle and a jaw morphology that is more suited for feeding on nectar rather than fruit (Mancina and Herrera 2010). The morphological peculiarities reported in *Brachyphylla*, within a clade comprising a broad array of specialist nectarivores, could be the result of dietary changes to exploit potential frugivore niches

left unoccupied by other phyllostomid bats during the Antilles colonization, as suggested by Griffiths (1985). This case illustrates only one of various examples of species exhibiting peculiar morphologies and exploiting a relatively unique niche within the same clade during the adaptive radiation of the Phyllostomidae, and might help explain differences in the covariance patterns observed from intraclade comparisons (see also Monteiro and Nogueira 2010).

Additionally, our results indicated substantial divergence in covariance patterns within comparisons between phylogenetically distant species (interclade comparisons) and those species exhibiting extreme phenotypes. For instance, pairwise comparisons involving *C. mexicana* and *C. senex* were more dissimilar than average, exhibiting the least similarities among phyllostomids (Fig. 2 and Table S5). The smallest values observed in our study are comparable to those found among the Old World Monkeys represented by *Miopithecus*, *Papio*, *Mandrillus*, *Homo*, *Gorilla*, and *Nomascus*, species that show remarkable cranial morphological disparity within catarrhines (see Oliveira et al. 2009). Unsurprisingly, the Mexican long-tongued bat *C. mexicana* and the wrinkle-faced bat *C. senex* are opposite extremes in terms of skull morphologies (Fig. 5). Exhibiting an extremely short and wide skull, *C. senex* is an obligate frugivore (Gardner 2008; Goodwin and Greenhall 1961) specialized in feeding on hard fruits. This species produces the strongest bite forces known among fruit-eating phyllostomid bats (Dumont et al. 2009). Conversely, the specialized nectar-feeding bat, *C. mexicana*, possesses a longer rostrum, which accounts for 40–50% of cranium length and a long tongue that measures ∼1/3 of its body length (Arroyo-Cabrales et al. 1987). *C. senex* displayed the lowest similarities in matrix comparisons, deviating largely from the covariance and correlation patterns shared by all other phyllostomid species. Monteiro and Nogueira (2010) investigated the relative importance of ecological and developmental factors in controlling patterns of within-species and evolutionary integration in the mandible of phyllostomid bats. They reported similar differences in within-species phenotypic integration patterns between clades representing different dietary groups.

Overall, our results complement previous empirical works reporting both the stability of the covariance structure at larger scales for mammals (Ackermann and Cheverud 2000; Marroig and Cheverud 2001; Ackermann 2002; Goswami 2006b; von Cramon-Taubadel et al. 2007; Oliveira et al. 2009; Porto et al. 2009; Garcia et al. 2014; Hubbe et al. 2016; von Cramon-Taubadel and Schroeder 2016; Machado et al. 2018; Sodini et al. 2018), as well as the divergence of some genera (Oliveira et al. 2009; Shirai and Marroig 2010; Hubbe et al. 2016) and families (Haber 2015; Machado et al. 2018).

These results discussed in the section above are based on the 48 within-species covariance matrices estimates and, therefore, reflects the distribution of the integration patterns of the currently recognized subfamilies of Phyllostomidae. However, considering the whole phylogeny, how are those differences distributed?

WHERE IN THE PHYLOGENY THE DISPARITY IS CONCENTRATED? THE PHYLOGENETIC STRUCTURE OF MORPHOLOGICAL INTEGRATION SPACE

The diversity decomposition analyses rejected the null hypothesis of random structure and indicated that both morphological integration patterns and magnitudes diverged early in the history of the Phyllostomidae (Fig. 5A and B, Table 3). The highly significant phylogenetic signal for all spaces tested (Table 3), emphasizes the importance of evolutionary history in the evolution of the covariance structure during phyllostomid diversification. This pattern of phylogenetic structuring among variables is reinforced by the results of matrix correlation (Table 1). Also, the association of phylogenetic history with covariance patterns was previously demonstrated between taxa (Ackermann 2002; Ackermann and Cheverud 2002; Goswami 2006b; Oliveira et al. 2009; Haber 2015), and among populations of the same subspecies (Steppan 1997).

The largest variation in integration patterns was significantly concentrated in the transition to three major clades: Glossophaginae (nectarivory), Lonchorhininae (strict insectivory) and Lonchophyllinae (nectarivory) (Fig. 5A). Other instances of significant variation were detected in the divergence of clades comprising frugivorous, obligate frugivorous and carnivorous bats (Fig. 5A). For integration magnitudes, the largest variation seems to be associated with the split of major clades that resulted in the remarkable feeding specializations currently recognized (Fig. 5B). Additionally, significant variation for integration magnitude was found in the divergence of clades comprising frugivorous, obligate frugivorous and omnivorous bats (Fig. 5B).

TEMPO OF THE MORPHOLOGICAL INTEGRATION EVOLUTION

DTT analyses allowed the evaluation of temporal variation in the patterns and magnitudes of integration (Figs. 6A and 6B). We observed that while the integration patterns were relatively stable through time, with almost constant average disparities (Fig. 6A), the magnitude showed remarkable variation over the course of evolution (Fig. 6B). These results complement previous large-scale studies investigating morphological integration in several mammalian orders (Cheverud 1996b; Ackermann and Cheverud 2000; Marroig and Cheverud 2001; Goswami 2006b; Oliveira et al. 2009; Porto et al. 2009, 2015; Haber 2015; Hubbe et al. 2016). Three significant decreases in magnitude were observed which were associated with important dietary transitions and the emergence of novel clades. The first occurred at the beginning of phyllostomid diversification (approx. 27-23 Myr), and

coincides with the phenotypic (shape and size) and ecological (diet) divergence previously reported by Monteiro and Nogueira (2011). This period is marked by a transition in multiple species from a primarily insectivorous ancestral feeding habit to a feeding habit which also included plant material (Ferrarezi and Gimenez 1996; Freeman 2000; Baker et al. 2012). This change in feeding ecology has been hypothesized to have reduced competition with other insectivorous bat species (Freeman 2000; Baker et al. 2012), and set the stage for the successful diversification of Phyllostomidae. The second decrease is coincident with evolution into different dietary adaptive zones and the radiation of several clades (between approximately 24-20 Myr), and the third decrease (~9 Myr) is coincident with the radiation of the short-faced bats, subtribe Stenodermatina (Fig. 5 and 7B). This clade evolved from a primarily frugivorous ancestor into highly specialized frugivores. This radiation into the obligate frugivory niche was preceded by intense selection (Rossoni et al. 2017) and represents the most recent burst of diversification in the Phyllostomidae (Rojas et al. 2016).

IS THE EVOLUTION OF MORPHOLOGICAL INTEGRATION IN PHYLLOSTOMID BATS ASSOCIATED WITH DIETARY SPECIALIZATIONS AND ROOSTING ECOLOGY?

Several studies on phyllostomid radiation have focused on the relationships between feeding behavior and trophic morphology (*e.g.*, Wetterer et al. 2000; Datzmann et al. 2010; Dumont et al. 2011; Monteiro and Nogueira 2011; Rojas et al. 2011). Monteiro and Nogueira (2010) reported a strong association between diet, shape, and phylogenetic distance in the phyllostomid mandible. An overview of the current clades comprising the family Phyllostomidae supports direct evidence of these associations between phylogeny, roosting, dietary habits, and morphology (Fig. 5). Kunz and Lumsden (2003) discussed how roost availability could influence both social organization and dietary strategy in bats. They argue that roosting ecology may be understood as a complex interaction of both biotic and abiotic variables, and roosting strategies may be directly influenced by the distribution and availability of food resources, among other things (Kunz and Lumsden 2003). Previous works have demonstrated that traits associated with roosting ecology might explain some morphological variation seen in phyllostomids (Garbino and Tavares 2018; Santana et al. 2011). Additionally, Tavares et al. (2018) proposed that traits associated with roosting behavior might have played an important role during the diversification of short-faced bats on the mainland.

Given the importance of these ecological variables for Phyllostomidae morphological evolution, is easy to predict that they might have played a role in influencing the evolution of the covariance structure. So far, the results from diversity decomposition, DTT analysis and matrix comparisons strongly suggested the influence of ecology in modifying the cranial morphological integration in phyllostomid bats. Matrices correlation results not only showed a significant association between morphological integration and ecological variables, as indicated the presence of strong phylogenetic structuring in these variables (Table 1). The degree of phylogenetic structuring among morphological integration patterns, morphology and the ecological variables is quite evident when represented using phylomorphospaces on the PCoord axes (Fig. 7). These plots illustrate that, in terms of ecology, closely related taxa tended to cluster together in similar regions of morphospace, while more distant taxa were distributed further from one another in more disparate regions of morphospace (Fig. 7). Correlation matrices results also indicated that species with similar feeding specializations shared similar roosting habits ($r = 0.59$, $p < 0.001$; Table 2). Diet and roosting were also significantly associated with average morphology ($r = 0.32$ and $r = 0.16$, $p < 0.001$), indicating that species with similar feeding and roosting behaviors are morphologically similar (Table 2).

Our results complement the studies reported above, demonstrating that feeding strategies and roosting ecology diversified together during phyllostomid evolutionary history, and explain a significant proportion of morphological evolution within clades. Additionally, our results extended these findings through a comparative quantitative genetic investigation of the evolution of the covariance structure, showing that the evolution of morphological integration in phyllostomid bats is associated with dietary specializations and roosting ecology (see next section below). Overall, it seems reasonable to argue that these two ecological factors (diet and roosting) were significant drivers of phyllostomid radiation, with their evolution being in close association with variation in integration structure (patterns and magnitude) as well as average morphological differentiation.

HAS MORPHOLOGICAL INTEGRATION CHANGED AS A BY-PRODUCT OF SELECTION ACTING IN SPECIES AVERAGE MORPHOLOGY?

The quantitative genetic theory predicts that the covariance structure might change indirectly or directly in response to natural selection. Indirect changes in covariance structure might result from selection acting to differentiate species average morphology, indirectly changing variances and covariances among traits (*i.e.*, the covariance change as a by-product of changes in species average morphology). Direct changes might result from selection acting directly upon both the variances and covariances among traits; not necessarily affecting the mean phenotype. Studying relationship QTLs (rQTLs), Pavlicev et al. (2008, 2011) identified "neutral" rQTLs capable to change the variance and covariance among traits without affect the trait means. These studies highlight the importance of epistatic pleiotropy in shaping covariation (see also Wolf et al. 2005).

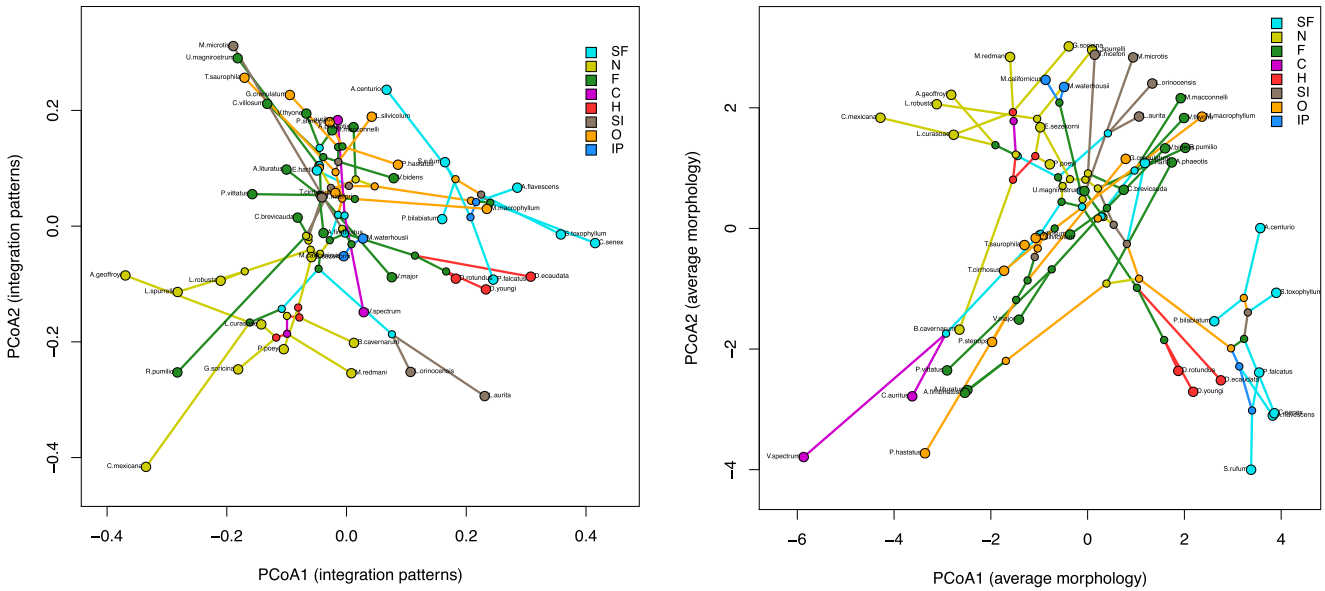

Figure 7. Phylomorphospaces plot viewed as the first two principal coordinates of the integration patterns (*RSDis*) and morphological differentiation (*MorphDis*). Labels represent dietary strategies in phyllostomid bats (SF, strict frugivory; N, nectarivory; F, frugivory; C, carnivory; H, hematophagy; SI, strict insectivory; O, omnivory; IP, insectivory). Colors presented here match those of the Figure 5.

In our study, matrix correlation results revealed a significant association between morphological integration patterns (*RSDis*) and morphological differentiation (*MorphDis*) (Table 1), suggesting a coordinated evolution of both trait averages and phenotypic covariances throughout clade diversification. This association suggests that natural selection had two potential roles in changing morphological integration during phyllostomid diversification. Firstly, directional selection resulting in the differentiation of species average morphology (see Rossoni et al. 2017) may have had indirect consequences on the shaping of cranial inter-trait relationships in phyllostomid bats. Alternatively, directional selection may have acted directly upon both trait averages and covariances during phyllostomid diversification. Although the first scenario (indirect changes) seems more reasonable, given that the greater the cranial morphological divergence in phyllostomid bats, the greater the dissimilarity in their covariance matrices, it does not explain all the divergence observed in our data. Probably, both scenarios happened during phyllostomid diversification. Morphological integration might have changed as a by-product of selection acting in species average morphology, and also, selection might have acted directly on variances and covariances to change functional and developmental morphological integration patterns associated with ecological adaptations (this will be investigated in a future contribution).

Remarkably, our results suggested that an evolutionary model of adaptation with multiple peaks corresponding to species occupying different dietary and roosting adaptive zones was the most likely scenario for the evolution of morphological integration structure and average morphological differentiation in phyllostomid bats (Tables SI2-1 and SI2-2; Figs. SI2-1A,C and SI2-1A,B). Macroevolution in phyllostomids might conform with Simpson's phenotypic landscape hypothesis based on dynamics among adaptive zones (Simpson 1944, 1953). According to Simpson (1944, 1953), the evolution of appropriate traits, *i.e.*, those that meet functional demands, could facilitate an organism in accessing and occupying a new adaptive zone. Our results demonstrate that ascending those novel dietary and roosting peaks (Simpsonian subzones; Simpson 1944) involved changes in morphological integration structure (phenotypic covariance patterns and magnitudes) and morphological differentiation (average morphology) during the diversification of phyllostomids (see also Pfaender et al. 2016). In a previous study, we have also demonstrated that natural selection was the key process driving phyllostomid diversification by directly affecting cranial morphology (Rossoni et al. 2017). Moreover, by reconstructing selection gradients along the phylogeny, we have shown that intense magnitudes of selection preceded invasions of new ecological niches and the appearance of novel feeding specializations (Rossoni et al. 2017). Based upon theoretical models, Pavlicev and co-workers (2011) demonstrated that directional selection can play an important role in changing genetic covariance patterns. Recent simulation approaches broadly supported this model (Jones et al. 2014; Melo and Marroig 2015), and empirical studies have demonstrated that directional selection can change patterns of integration in the mammalian skull, both in the wild (Assis et al. 2016) and in the laboratory (Penna et al. 2017).

Previous studies using phylogenetic comparative methods to investigate biomechanical performance (Dumont et al. 2014) and

mandible shape and size (Monteiro and Nogueira 2011) in phyllostomid bats have also found the Ornstein-Uhlenbeck process to be the best-supported evolutionary model for average morphology. Additionally, Dumont et al. (2012) demonstrated that changes in skull morphology enabled the expansion of dietary niches in stenodermatines. This clade includes the greatest relative numbers of genera and species in Phyllostomidae, with feeding strategies ranging from primary to obligate frugivory (Baker et al. 2012, see Fig. 5). The origin of this clade was associated with a significant increase in the rate of species diversification (Dumont et al. 2012) and with a strong magnitude of selection in the branch leading to highly specialized frugivores (the short-faced bats, Subtribe Stenodermatina) (Rossoni et al. 2017). Overall, our results extend those findings through a comparative quantitative genetic investigation, incorporating the covariance among traits, and leading to significant insights into the evolution of morphological integration in the most noteworthy example of adaptive radiation in mammals. Here, the interplay between natural selection, changes in the phenotypic covariance structure, and in trait averages (morphology), together with the invasion of novel dietary and roosting-based adaptive zones, can be thought of as having "fine-tuned" this adaptive radiation.

ARE THE COVARIANCE PATTERNS OF PARTICULAR TRAITS ASSOCIATED WITH DIET AND ROOSTING?

In analyzing the relationships between ecological variables and the covariance patterns of individual traits (SRD method; Marroig et al. 2011), our results revealed that dietary strategies and roosting ecologies are associated with covariance patterns in particular cranial traits, most of them associated with the oral, nasal, and zygomatic subregions (face region) and a some associated with vault and base subregions (neurocranial region) (Fig. 4, Tables S13 and S14). Especially for the face, traits that displayed significant correlation with feeding strategies also exhibited significant correlation with roosting ecology, and thus might indicate morphological correlates of dietary and roosting adaptations. Bats of the Subfamily Stenodermatinae are a good example of species sharing feeding strategies and roosting behaviors (see Fig. 5). This Subfamily contains bats that mostly feed on fruits, including almost all phyllostomid species known to roost in foliage and species known to modify leaves into tent shelters (Voss et al. 2016; Fig. 5). Feeding on fruits and changing the shape of leaves to create tent shelters involve biting through resistant plant tissues. These strategies and their associated physical challenges might demand biomechanical functions from the different regions of the skull. In the insectivorous bat *Lophostoma silvicolum*, for example, teeth are essential in the excavation of roosts in active termite nests (Kalko et al. 2006; Dechmann et al. 2009). This species generates high bite forces during biting behaviors associated with feeding and roost excavation (Dechmann et al. 2009). In our study, the landmarks involved in the SRD results mostly capture distances related to rostrum and palate extension and retraction (face region), being associated with the premaxilla, palate, and nasal bones (Fig. 4, Tables S13 and S14). These bones and associated muscle mechanics are strongly associated with biting performance (see Nogueira et al. 2009; Santana et al. 2010, 2012; Dumont et al. 2014). Regarding the neurocranium, the landmark APET is located in the basicranial subregion, and is also positioned close to the auditory region, which is host to the balance and orientation organs and additionally delimits the basisphenoid and basioccipital bones. The distance BRAPET for instance is associated with the vault subregion and, among other things, reflects the height of the braincase, which may vary greatly among species according to their feeding or roosting specializations and distinct morphologies. An interesting follow-up to our work would be to examine cranial modularity in phyllostomid bats, including hypotheses linking the functional demands of different dietary and roosting specializations with integration patterns and magnitudes. This approach would be advantageous in developing our understanding of the relative role of external factors as determinants of phenotypic covariance structure. Additionally, moving from one adaptive peak to another in the adaptive landscape might require substantial changes in the functional requirements of the phyllostomid skull (Dumont et al. 2014). Therefore, another important avenue for future research would be to quantify the functional performance in phyllostomid skulls and/or mandibles to investigate if the direction of selection and the direction of evolutionary response are aligned with biomechanical variables during dietary transitions along the phylogenetic tree, and whether these interactions have impacted integration structure.

Conclusion

In this study, we demonstrated that, on a broader phylogenetic scale, cranial morphological integration structure remained relatively similar during the evolution of the New World leaf-nosed bats. However, despite this overall similarity, we also observed substantial divergences between interclade comparisons. We found a significant degree of phylogenetic signal in all variables analyzed, emphasizing the importance of evolutionary history in dictating changes in morphological integration structure, feeding strategies, roosting ecologies, and morphological differentiation during phyllostomid diversification. Most of the phylogenetic structure in the integration space can be explained by splits at the beginning of the diversification of major clades in the Phyllostomidae. The adaptive radiation of phyllostomid bats was triggered by the diversification of dietary and roosting strategies, and the invasion of new adaptive zones leading to changes in phenotypic covariance structure and cranial morphology. In this scenario, intense natural selection preceded the

invasion of these new adaptive zones (at least for feeding strategies, see Rossoni et al. 2017) and played an important role in shaping both cranial covariance structure and morphological differentiation throughout the successful radiation of this hyperdiverse clade of mammals.

AUTHOR CONTRIBUTIONS

D.M.R. and G.M. conceived the study; D.M.R. collected data; D.M.R., B.M.A.C. and G.M. designed the analysis; D.M.R. performed the analysis and wrote the main manuscript; D.M.R., B.M.A.C., G.M. and N.P.G. contributed to the discussion of the results and the writing of the manuscript.

ACKNOWLEDGMENTS

We are grateful to all of the curators, faculty, and staff of the following institutions who provided generous help and access to the specimens used in this study: Mário de Vivo e Juliana Gualda (Museu de Zoologia da Universidade de São Paulo, MZUSP); Eliana Morielle Versute (Coleção de Chiroptera na UNESP de São José do Rio Preto, DZSJRP); João Alves e Stella Franco (Museu Nacional, MN); Sueli Marques Aguiar e José de Souza Júnior (Museu Paraense Emílio Goeldi, MPEG); Bruce Patterson, Lawrence Heaney e Bill Stanley (*in memoriam*) (Field Museum of Natural History, FMNH); Kristofer Helgen, Darrin Lunde, Marissa Atmann e Suzanne Peurach (National Museum of Natural History, NMNH); Nancy Simmons, Robert Voss e Eileen Westwig (American Museum of Natural History, AMNH); Robert Baker (*in memoriam*) e Heath Garner (Museum of Texas Tech University, TTU); and Jim Patton, Eileen Lacey e Chris Conroy (Museum of Vertebrate Zoology, MVZ). We thank Elizabeth Dumont and the University of Massachussets, Amherst, for providing support during the international internship of D.M.R. We thank Arthur Porto and all colleagues from our laboratory for their valuable comments to early versions of the manuscript. We thank Ana Paula Assis for help with the figure 4, Fábio Machado for help with figure 3 and Vitor Aguiar for facilitating the network server access. We thank Fábio Machado and Thiago Zahn for productive discussions on phylogenetic comparative methods. We thank the four anonymous reviewers and Liliana Dávalos for their comments and suggestions to improve the manuscript. We also would like to thank the Associate Editor Dr. Miriam Zelditch and the Handling Editor Dr. Maria Servidio for the editorial assistance on our manuscript. Financial support for this research was provided by Fundação de Amparo à Pesquisa do Estado de São Paulo—FAPESP (grants 2014/12632-4 to D.M.R.; 2015/16598-8 to B.M.A.C.; and 2011/14295-7 to G.M.), Coordenação de Aperfeiçoamento de Pessoal de Nível Superior—CAPES (grant 1072/11-0 to D.M.R. and 1602224 to B.M.A.C.) and grant PICT 2015-2389 to N.P.G.

DATA ARCHIVING

All data associated with this manuscript are available as supplementary files. Data is also available on the Dryad Digital Repository: https://doi.org/10.5061/dryad.78276h1.

CONFLICT OF INTEREST

The authors have no conflict of interest.

LITERATURE CITED

Ackermann, R. R. 2002. Patterns of covariation in the hominoid craniofacial skeleton: implications for paleoanthropological models. J. Hum. Evol. 43:167–187.

Ackermann, R. R., and J. M. Cheverud. 2000. Phenotypic covariance structure in tamarins (genus Saguinus): a comparison of variation patterns using matrix correlation and common principal component analysis. Am. J. Phys. Anthropol. 111:489–501.

———. 2002. Discerning evolutionary processes in patterns of tamarin (genus Saguinus) craniofacial variation. Am. J. Phys. Anthropol. 117: 260–271.

Arnold, S. J. 1981. Behavioral variation in natural populations. I. Phenotypic, genetic and environmental correlations between chemoreceptive responses to prey in the garter snake, Thamnophis elegans. Evolution 35:489–509.

———. 1992. Constraints on phenotypic evolution. Am. Nat. 140:85–107.

Arnold, S. J., and P. C. Phillips. 1999. Hierarchical comparison of genetic variance-covariance matrices. II. Coastal-inland divergence in the garter snake, Thamnophis elegans. Evolution 53:1516–1527. https://doi.org/10.2307/2640897.

Arnold, S. J., R. Bürger, P. A. Hohenlohe, B. C. Ajie, and A. G. Jones. 2008. Understanding the evolution and stability of the G-matrix. Evolution 62:2451–2461.

Arroyo-Cabrales, J., R. R. Hollander, and J. J. Knox Jones. 1987. *Choeronycteris mexicana*. Species 291:1–5.

Assis, A. P. A., J. L. Patton, A. Hubbe, and G. Marroig. 2016. Directional selection effects on patterns of phenotypic (co)variation in wild populations. Proc. R. Soc. B Biol. Sci. 283:20161615.

Baker, R. J., S. Hoofer, C. Porter, and R. Van Den Bussche. 2003. Diversification among New World leaf-nosed bats: an evolutionary hypothesis and classification inferred from digenomic congruence of DNA sequence. Occas. Pap. Mus. Tex. Tech Univ. 230:1–32.

Baker, R. J., O. R. P. Bininda-Emonds, H. Mantilla-Meluk, C. A. Porter, and R. A. Van Den Bussche. 2012. Molecular time scale of diversification of feeding strategy and morphology in New World Leaf-Nosed Bats (Phyllostomidae): a phylogenetic perspective. Pp. 385–409 *in* G. F. Gunnell and N. B. Simmons, eds. Evolutionary history of bats. Cambridge Univ. Press, Cambridge, U.K.

Blows, M. W., and M. Higgie. 2003. Genetic constraints on the evolution of mate recognition under natural selection. Am. Nat. 161:240–253.

Blows, M. W., S. F. Chenoweth, and E. Hine. 2004. Orientation of the genetic variance-covariance matrix and the fitness surface for multiple male sexually selected traits. Am. Nat. 163:329–340.

Cheverud, J. M. 1982. Phenotypic, genetic, and environmental morphological integration in the cranium. Evolution 36:499–516.

———. 1988. A comparison of genetic and phenotypic correlations. Evolution 42:958–968.

———. 1995. Morphological integration in the saddle-back tamarin (*Saguinus fuscicollis*) cranium. Am. Nat. 145:63–89.

———. 1996a. Developmental integration and the evolution of pleiotropy. Am. Zool. 36:44–50.

———. 1996b. Quantitative genetic analysis of cranial morphology in the cotton-top (*Saguinus oedipus*) and saddle-back (*S. fuscicollis*) tamarins. J. Evol. Biol. 9:5–42.

Cheverud, J. M., and G. Marroig. 2007. Comparing covariance matrices: Random Skewers method compared to the common principal components model. Genet. Mol. Biol. 30:461–469.

Cheverud, J. M., G. P. Wagner, and M. M. Dow. 1989. Methods for the comparative analysis of variation patterns. Evolution 38:201–213.

Clavel, J., G. Escarguel, and G. Merceron. 2015. MVMORPH: an R package for fitting multivariate evolutionary models to morphometric data. Methods Ecol. Evol. 6:1311–1319.

Datzmann, T., O. von Helversen, and F. Mayer. 2010. Evolution of nectarivory in phyllostomid bats (Phyllostomidae Gray, 1825, Chiroptera: Mammalia). BMC Evol. Biol. 10:165.

Dechmann, D. K. N., S. E. Santana, and E. R. Dumont. 2009. Roost making in bats—adaptations for excavating active termite nests. J. Mammal. 90:1461–1468.

Dow, M. M., and J. M. Cheverud. 1985. Comparison of distance matrices in studies of population structure and genetic microdifferentiation: quadratic assignment. Am. J. Phys. Anthropol. 68:367–373.

Dumont, E. R., A. Herrel, R. A. Medellín, J. A. Vargas-Contreras, and S. E. Santana. 2009. Built to bite: cranial design and function in the wrinkle-faced bat. J. Zool. 279:329–337.

Dumont, E. R., L. M. Davalos, A. Goldberg, S. E. Santana, K. Rex, and C. C. Voigt. 2011. Morphological innovation, diversification and invasion of a new adaptive zone. Proc. R. Soc. B Biol. Sci. 279:1797–1805.

Dumont, E. R., K. Samadevam, I. Grosse, O. M. Warsi, B. Baird, and L. M. Davalos. 2014. Selection for mechanical advantage underlies multiple cranial optima in New World leaf-nosed bats. Evolution 68:1436–1449.

Edwards, D. L., J. Melville, L. Joseph, and J. S. Keogh. 2015. Ecological divergence, adaptive diversification, and the evolution of social signaling traits: an empirical study in arid Australian lizards. Am. Nat. 186:E144–E161.

Evans, M. E. K., S. A. Smith, R. S. Flynn, and M. J. Donoghue. 2009. Climate, niche evolution, and diversification of the "bird-cage" evening primroses (*Oenothera*, sections *Anogra* and *Kleinia*). Am. Nat. 173: 225–240.

Ferrarezi, H., and E. Gimenez. 1996. Systematic patterns and the evolution of feeding habits in Chiroptera (Archonta: Mammalia). J. Comp. Biol. 1:75–94.

Freeman, P. W. 1995. Nectarivorous feeding mechanisms in bats. Biol. J. Linn. Soc. 56:439–463.

———. 1998. Form, function, and evolution in skulls and teeth of bats. Pp. 140–156 *in* T. H. Kunz and P. A. Racey, eds. Bat biology and conservation. Smithsonian Institution Press, Washington, DC.

———. 2000. Macroevolution in microchiroptera: recoupling morphology and ecology with phylogeny. Evol. Ecol. Res. 2:317–335.

Garbino, G. S. T., and V. da C. Tavares. 2018. Roosting ecology of Stenodermatinae bats (Phyllostomidae): evolution of foliage roosting and correlated phenotypes. Mammal Rev. 48:75–89.

Garcia, G., E. Hingst-Zaher, R. Cerqueira, and G. Marroig. 2014. Quantitative genetics and modularity in cranial and mandibular morphology of *Calomys expulsus*. Evol. Biol. 41:619–636.

Gardner, A. L., ed. 2007. Mammals of South America. University of Chicago Press, Chicago, IL.

———. 2008. Mammals of South America. University of Chicago Press, Chicago, IL.

Giannini, N. P., and E. K. Kalko. 2004. Trophic structure in a large assemblage of phyllostomid bats in Panama. Oikos 105:209–220.

Goodwin, G., and A. Greenhall. 1961. A review of the bats of Trinidad and Tobago. Bull. Am. Mus. Nat. Hist. 122:187–301.

Goswami, A. 2006a. Cranial modularity shifts during mammalian evolution. Am. Nat. 168:270–280.

———. 2006b. Morphological integration in the carnivoran skull. Evolution 60:169–183.

Griffiths, T. A. 1985. Molar cusp patterns in the bat genus brachyphylla: some functional and systematic observations. J. Mammal. 66:544–549.

Haber, A. 2015. The evolution of morphological integration in the ruminant skull. Evol. Biol. 42:99–114.

Harmon, L. J., and R. E. Glor. 2010. Poor statistical performance of the Mantel test in phyllogenetic comparative analysis. Evolution, https://doi.org/10.1111/j.1558-5646.2010.00973.x.

Hansen, T. F., and D. Houle. 2008. Measuring and comparing evolvability and constraint in multivariate characters. J. Evol. Biol. 21:1201–1219.

Harmon, L. J., J. A. Schulte, A. Larson, and J. B. Losos. 2003. Tempo and mode of evolutionary radiation in iguanian lizards. Science 301:961–964.

Harmon, L. J., J. T. Weir, C. D. Brock, R. E. Glor, and W. Challenger. 2008. GEIGER: investigating evolutionary radiations. Bioinformatics 24:129–131.

Harmon, L. J., J. B. Losos, T. Jonathan Davies, R. G. Gillespie, J. L. Gittleman, W. Bryan Jennings, K. H. Kozak, M. A. McPeek, F. Moreno-Roark, T. J. Near, et al. 2010. Early bursts of body size and shape evolution are rare in comparative data. Evolution 64:2385–2396.

Hubbe, A., D. Melo, and G. Marroig. 2016. A case study of extant and extinct Xenarthra cranium covariance structure: implications and applications to paleontology. Paleobiology 42:465–488.

Jamniczky, H. A., and B. Hallgrímsson. 2009. A comparison of covariance structure in wild and laboratory muroid crania. Evolution 63:1540–1556.

Jones, A. G. 2007. The mutation matrix and the evolution of evolvability. Evolution 61:727–745.

Jones, A. G., S. J. Arnold, and R. Burger. 2003. Stability of the G-matrix in a population experiencing pleiotropic mutation, stabilizing selection, and genetic drift. Evolution 57:1747–1760.

———. 2004. Evolution and stability of the G-matrix on a landscape with a moving optimum. Evolution 58:1639–1654.

Jones, A. G., R. Bürger, S. J. Arnold, P. A. Hohenlohe, and J. C. Uyeda. 2012. The effects of stochastic and episodic movement of the optimum on the evolution of the G-matrix and the response of the trait mean to selection. J. Evol. Biol. 25:2210–2231.

Jones, A. G., R. Bürger, and S. J. Arnold. 2014. Epistasis and natural selection shape the mutational architecture of complex traits. Nat. Commun. 5:3709.

Kalko, E. K. V., K. Ueberschaer, and D. Dechmann. 2006. Roost structure, modification, and availability in the white-throated round-eared bat, *Lophostoma silvicolum* (Phyllostomidae) living in active termite nests1: roosting ecology of *L. silvicolum* in Panamá. Biotropica 38:398–404.

Klingenberg, C. P. 2014. Studying morphological integration and modularity at multiple levels: concepts and analysis. Philos. Trans. R. Soc. B Biol. Sci. 369:20130249–20130249.

Kruuk, L. E. B., J. Slate, and A. J. Wilson. 2008. New answers for old questions: the evolutionary quantitative genetics of wild animal populations. Annu. Rev. Ecol. Evol. Syst. 39:525–548.

Krzanowsky, W. J. 1979. Between-groups comparison of principal components. J. Am. Stat. Assoc. 74:703–707.

Kunz, T. H., and L. F. Lumsden. 2003. Ecology of cavity and foliage roosting bats. Pp. 3–89 *in* T.H. Kunz and M.B. Fenton, eds. Bat ecology. University of Chicago Press, Chicago, IL.

Lande, R. 1979. Quantitative genetic analysis of multivariate evolution applied to brain: body size allometry. Evolution 33:402–416.

Lande, R., and S. J. Arnold. 1983. The measurement of selection on correlated characters. Evolution 37:1210–1226.

Lessels, C. M., and P. T. Boag. 1987. Unrepeatable repeatabilities: a common mistake. Auk 2:116–121.

Machado, F. A., T. M. G. Zahn, and G. Marroig. 2018. Evolution of morphological integration in the skull of Carnivora (Mammalia): changes in Canidae lead to increased evolutionary potential of facial traits. Evolution 72:1399–1419.

Mancina, Carlos A., and L. Gerardo Herrera M. 2010. Disparate feeding strategies used by syntopic Antillean nectarivorous bats to obtain dietary protein. Journal of Mammalogy 91:960–966. https://doi.org/10.1644/09-mamm-a-323.1.

Mantel, N. 1967. The detection of disease clustering and a generalized regression approach. Cancer Res. 27:209–220.

Marroig, G., and J. M. Cheverud. 2001. A comparison of phenotypic variation and covariation patterns and the role of phylogeny, ecology, and ontogeny during cranial evolution of new world monkeys. Evolution 55:2576–2600.

Marroig, G., and J. Cheverud. 2010. Size as a line of least resistance II: direct selection on size or correlated response due to constraints? Evolution: International Journal of Organic Evolution 64:1470–1488. https://doi.org/10.1111/j.1558-5646.2009.00920.x.

Marroig, G., D. Melo, A. Porto, H. Sebastião, and G. Garcia. 2011. Selection Response Decomposition (SRD): a new tool for dissecting differences and similarities between matrices. Evol. Biol. 38:225–241.

Melo, D., G. Garcia, A. Hubbe, A. P. Assis, and G. Marroig. 2015. EvolQG—an R package for evolutionary quantitative genetics. F1000Res. 4:925.

Melo, D., and G. Marroig. 2015. Directional selection can drive the evolution of modularity in complex traits. Proc. Natl. Acad. Sci. 112:470–475.

Mitteroecker, P., and F. L. Bookstein. 2008. The evolutionary role of modularity and integration in the hominoid cranium. Evolution 62:943–958.

———. 2009. The ontogenetic trajectory of the phenotypic covariance matrix, with examples from craniofacial shape in rats and humans. Evolution 63:727–737.

Monteiro, L. R., and M. R. Nogueira. 2010. Adaptive radiations, ecological specialization, and the evolutionary integration of complex morphological structures. Evolution 64:724–744.

———. 2011. Evolutionary patterns and processes in the radiation of phyllostomid bats. BMC Evol. Biol. 11:1.

Nogueira, M. R., A. L. Peracchi, and L. R. Monteiro. 2009. Morphological correlates of bite force and diet in the skull and mandible of phyllostomid bats. Funct. Ecol. 23:715–723.

Nowak, R. M., and E. P. Walker. 1994. Walker's bats of the world. Johns Hopkins Univ. Press, Baltimore, MD.

Oliveira, F. B., A. Porto, and G. Marroig. 2009. Covariance structure in the skull of Catarrhini: a case of pattern stasis and magnitude evolution. J. Hum. Evol. 56:417–430.

Paradis, E., J. Claude, and K. Strimmer. 2004. APE: analyses of phylogenetics and evolution in R language. Bioinformatics 20:289–290.

Pavlicev, M., J. P. Kenney-Hunt, E. A. Norgard, C. C. Roseman, J. B. Wolf, and J. M. Cheverud. 2008. Genetic variation in pleiotropy: differential epistasis as a source of variation in the allometric relationship between long bone lengths and body weight. Evolution 62:199–213.

Pavlicev, M., J. M. Cheverud, and G. P. Wagner. 2009. Measuring morphological integration using eigenvalue variance. Evol. Biol. 36:157–170.

Pavlicev, M., E. A. Norgard, G. L. Fawcett, and J. M. Cheverud. 2011. Evolution of pleiotropy: epistatic interaction pattern supports a mechanistic model underlying variation in genotype-phenotype map. J. Exp. Zool. B 316:371–85.

Pavoine, S., M. Baguette, and M. B. Bonsall. 2010. Decomposition of trait diversity among the nodes of a phylogenetic tree. Ecol. Monogr. 80:23.

Pedersen, S. C., and R. Müller. 2013. Nasal-emission and nose leaves. Pp. 71–91 *in* R. A. Adams and S. C. Pedersen, eds. Bat evolution, ecology, and conservation. Springer, New York, NY.

Penna, A., D. Melo, S. Bernardi, M. I. Oyarzabal, and G. Marroig. 2017. The evolution of phenotypic integration: how directional selection reshapes covariation in mice. Evolution 71:2370–2380.

Pfaender, J., R. K. Hadiaty, U. K. Schliewen, and F. Herder. 2016. Rugged adaptive landscapes shape a complex, sympatric radiation. Proc. R. Soc. B Biol. Sci. 283:20152342.

Pitchers, W. R., R. Brooks, M. D. Jennions, T. Tregenza, I. Dworkin, and J. Hunt. 2013. Limited plasticity in the phenotypic variance-covariance matrix for male advertisement calls in the black field cricket, *Teleogryllus commodus*. J. Evol. Biol. 26:1060–1078.

Porto, A., F. B. Oliveira, L. T. Shirai, V. de Conto, and G. Marroig. 2009. The evolution of modularity in the mammalian skull I: morphological integration patterns and magnitudes. Evol. Biol. 36:118–135.

Porto, A., L. T. Shirai, F. B. de Oliveira, and G. Marroig. 2013. Size Variation, Growth Strategies, and the Evolution of Modularity in the Mammalian Skull. Evolution 67:3305–3322.

Porto, A., H. Sebastião, S. E. Pavan, J. L. VandeBerg, G. Marroig, and J. M. Cheverud. 2015. Rate of evolutionary change in cranial morphology of the marsupial genus *Monodelphis* is constrained by the availability of additive genetic variation. J. Evol. Biol. 28:973–985.

Puentes, A., G. Granath, and J. Ågren. 2016. Similarity in G matrix structure among natural populations of *Arabidopsis lyrata*. Evolution 70:2370–2386.

R Core Team. 2018. R: a language and environment for statistical computing. R Foundation for Statistical Computing, Vienna, Austria.

Revell, L. J. 2007. The G matrix under fluctuating correlational mutation and selection. Evolution 61:1857–1872.

———. 2012. phytools: an R package for phylogenetic comparative biology (and other things): phytools: R package. Methods Ecol. Evol. 3:217–223.

Rodriguez, A., and L. Dávalos. 2008. Brachyphylla cavernarum. The IUCN Red List of Threatened Species 2008: e.T2982A9528532. https://doi.org/10.2305/IUCN.UK.2008.RLTS.T2982A9528532.en.

Rodríguez-H., B., R. A. Medellín, and R. M. Timm. 2007. Murciélagos neotropicales que acampan en hojas. 1st ed. Instituto Nacional de Biodiversidad, INBio, Santo Domingo de Heredia, Costa Rica.

Roff, D. 2000. The evolution of the G matrix: selection or drift? Heredity 84:135.

Roff, D. A. 1995. The estimation of genetic correlations from phenotypic correlations: a test of Cheverud's conjecture. Heredity 74:481–490.

———. 1996. The evolution of genetic correlations: an analysis of patterns. Evolution 50:1392–1403.

Rojas, D., A. Vale, V. Ferrero, and L. Navarro. 2011. When did plants become important to leaf-nosed bats? Diversification of feeding habits in the family Phyllostomidae: evolution of feeding habits in phyllostomid bats. Mol. Ecol. 20:2217–2228.

Rojas, D., O. M. Warsi, and L. M. Dávalos. 2016. Bats (Chiroptera: Noctilionoidea) challenge a recent origin of extant neotropical diversity. Syst. Biol. 65:432–448.

Roseman, C. C., T. D. Weaver, and C. B. Stringer. 2011. Do modern humans and Neandertals have different patterns of cranial integration? J. Hum. Evol. 60:684–693.

Rossoni, D. M., A. P. A. Assis, N. P. Giannini, and G. Marroig. 2017. Intense natural selection preceded the invasion of new adaptive zones during the radiation of New World leaf-nosed bats. Sci. Rep. 7:11076.

Santana, S. E., E. R. Dumont, and J. L. Davis. 2010. Mechanics of bite force production and its relationship to diet in bats. Funct. Ecol. 24:776–784.

Santana, S. E., T. O. Dial, T. P. Eiting, and M. E. Alfaro. 2011. Roosting ecology and the evolution of pelage markings in bats. PLoS ONE 6:e25845.

Santana, S. E., I. R. Grosse, and E. R. Dumont. 2012. Dietary hardness, loading behavior, and the evolution of skull form in bats. Evolution 66:2587–2598.

Schluter, D. 1996. Adaptive radiation along genetic lines of least resistance. Evolution 50:1766–1774.

Shirai, L. T., and G. Marroig. 2010. Skull modularity in neotropical marsupials and monkeys: size variation and evolutionary constraint and flexibility. J. Exp. Zoolog. B Mol. Dev. Evol. 314B:663–683.

Simmons, N. B. 2005. Order Chiroptera. Pp. 312–529 *in* Mammal species of the world: a taxonomic and geographic reference. Johns Hopkins Univ. Press, Baltimore, MD.

Simpson, G. G. 1944. Tempo and mode in evolution. Columbia Univ. Press, New York, NY.

———. 1953. The major features of evolution. Columbia Univ. Press, New York, NY.

Slater, G. J., and M. W. Pennell. 2014. Robust regression and posterior predictive simulation increase power to detect early bursts of trait evolution. Syst. Biol. 63:293–308.

Slater, G. J., S. A. Price, F. Santini, and M. E. Alfaro. 2010. Diversity versus disparity and the radiation of modern cetaceans. Proc. R. Soc. B Biol. Sci. 277:3097–3104.

Slater, G. J., J. A. Goldbogen, and N. D. Pyenson. 2017. Independent evolution of baleen whale gigantism linked to Plio-Pleistocene ocean dynamics. Proc. R. Soc. B Biol. Sci. 284:20170546.

Sodini, S. M., K. E. Kemper, N. R. Wray, and M. Trzaskowski. 2018. Comparison of genotypic and phenotypic correlations: Cheverud's conjecture in humans. Genetics, https://doi.org/10.1534/genetics.117.300630.

Steppan, S. J. 1997. Phylogenetic analysis of phenotypic covariance structure. I. Contrasting results from matrix correlation and common principal component analysis. Evolution 51:571–586.

Steppan, S. J., P. C. Phillips, and D. Houle. 2002. Comparative quantitative genetics: evolution of the G matrix. Trends Ecol. Evol. 17:320–327.

Tavares, V. da C., O. M. Warsi, F. Balseiro, C. A. Mancina, and L. M. Dávalos. 2018. Out of the Antilles: fossil phylogenies support reverse colonization of bats to South America. J. Biogeogr. 45:859–873.

Tukey, J. W. 1977. Exploratory data analysis. Addison-Wesley Pub. Co, Reading, MA.

Turelli, M. 1988. Phenotypic evolution, constant covariances, and the maintenance of additive variance. Evolution 42:1342–1347.

von Cramon-Taubadel, N., and L. Schroeder. 2016. Testing the equivalence of modern human cranial covariance structure: Implications for bioarchaeological applications: von C ramon -T aubadel and S chroeder. Am. J. Phys. Anthropol. 161:355–366.

von Cramon-Taubadel, N., B. C. Frazier, and M. M. Lahr. 2007. The problem of assessing landmark error in geometric morphometrics: theory, methods, and modifications. Am. J. Phys. Anthropol. 134:24–35.

Voss, R. S., D. W. Fleck, R. E. Strauss, P. M. Velazco, and N. B. Simmons. 2016. Roosting ecology of Amazonian bats: evidence for guild structure in hyperdiverse mammalian communities. Am. Mus. Novit. 3870:1–43.

Wetterer, A. L., M. V. Rockman, and N. B. Simmons. 2000. Phylogeny of phyllostomid bats (Mammalia: Chiroptera): data from diverse morphological systems, sex chromosomes, and restriction sites. Bulletin of the American Museum of Natural History 248:1–200, New York, NY.

Willmore, K. E., C. C. Roseman, J. Rogers, J. M. Cheverud, and J. T. Richtsmeier. 2009. Comparison of mandibular phenotypic and genetic integration between baboon and mouse. Evol. Biol. 36:19–36.

Wolf, J. B., L. J. Leamy, E. J. Routman, and J. M. Cheverud. 2005. Epistatic pleiotropy and the genetic architecture of covariation within early and late-developing skull trait complexes in mice. Genetics 171:683–94.

Yohe, L. R., R. Abubakar, C. Giordano, E. Dumont, K. E. Sears, S. J. Rossiter, and L. M. Dávalos. 2017. *Trpc2* pseudogenization dynamics in bats reveal ancestral vomeronasal signaling, then pervasive loss. Evolution 71:923–935.

Yohe, L. R., S. Hoffmann, and A. Curtis. 2018. Vomeronasal and olfactory structures in bats revealed by DiceCT clarify genetic evidence of function. Front. Neuroanat. 12:32.

Associate Editor: M. L. Zelditch
Handling Editor: M. R. Servedio

Supporting Information

Additional supporting information may be found online in the Supporting Information section at the end of the article.

Supporting Information